expected, NPC1 was absent in UCH cell fractions and, again unlike in H34 cells, SKD1 was not at all recovered in these fractions regardless of the cellular cholesterol levels.

It was possible that this lack of SKD1 recruitment in UCH cells was simply because the cells lacking NPC1 could not be effectively depleted of cholesterol. To address this issue, UCH cells were cultured in cholesterol-depleted medium for 3 days. This treatment abolished endosomal cholesterol accumulation as revealed by filipin staining but again failed to induce endosomal recruitment of SKD1 (data not shown). These findings suggested that the negative results in UCH cells were not a result of ineffective cholesterol depletion, but a result of the absence of NPC1.

Finally, to see if NPC2 is involved in the regulation of NPC1 ubiquitylation, we repeated the same experiments using cells from a patient with NPC2 disease (90031, homozygous for the NPC2 E20X mutation), which lack NPC2 function. Our previous analysis using 0.4% SDS extracts from 100,000 *g* membrane preparations revealed an increased amount of NPC1 in the NPC2 cells as compared with control cells (Millat et al., 2001a). However, anti-NPC1 blotting of 0.5% CHAPS extracts showed comparable levels of NPC1 between H34 and the NPC2 cells (Fig. 6A), suggesting reduced solubility of NPC1 in these cells to this detergent. Nonetheless, anti-ubiquitin immunoprecipitation experiments using the 0.5% CHAPS extracts revealed distinct patterns of NPC1 ubiquitylation. A part of NPC1 was ubiquitylated in these cells regardless of the cholesterol levels (Fig. 6B). This ubiquitylation of NPC1 was accompanied by the presence of SKD1 in the anti-ubiquitin immunoprecipitation products from cells cultured either in cholesterol-rich or cholesterol-depleted medium (Fig. 6B). Opti-prep fractionation of the NPC2 cells showed a distinct distribution pattern of SKD1. Both lamp2 and NPC1 were recovered in fractions 2 and 3 from cells cultured in cholesterol-rich medium and, unlike in H34 cells, cholesterol depletion caused a rightward shift of this distribution to fractions 3-5. In contrast to H34 cells, SKD1 co-localized with NPC1 regardless of the cellular cholesterol levels and it was present in fractions 2 and 3, and in 3-5, from cells cultured in cholesterol-rich and cholesterol-depleted medium, respectively (Fig. 6C). Similar results were obtained by using another NPC2 cell strain 88082 (data not shown), suggesting that they are a common feature of NPC2-deficient cells.

Discussion

The biochemical mechanism and physiological implication of the cholesterol-dependent control of protein ubiquitylation has so far been documented only for HMG-CoAR, a rate-limiting enzyme of cholesterol biosynthesis localized in the ER. Briefly, repletion of cellular cholesterol facilitates association of HMG-CoAR with the Insig proteins, which in turn accelerates its ubiquitylation and proteasomal degradation (Ravid et al., 2000; Sever et al., 2003a; Sever et al., 2003b). We have shown in the current study that ubiquitylation of NPC1 was induced by depletion of cellular cholesterol, but not by its repletion. It is currently unknown how cholesterol exerts opposite effects on NPC1 and HMG-CoAR, the two proteins that share SSDs. These opposite effects possibly result from differences in their subcellular locations and/or the nature of the interacting proteins involved in the regulatory processes. We have shown that two kinds of mutant NPC1 proteins – P691S and δLLNF – failed to respond to cholesterol depletion (Fig. 2). The negative response of the P691S mutant suggested that an intact SSD was required for NPC1 to undergo this modification, whereas the negative response of the δLLNF mutant suggested that the modification took place in the endosomes, where NPC1 normally resides.

Ubiquitylation of a protein can serve as a signal for its degradation or intracellular sorting. Unlike the case of HMG-CoAR, cholesterol-level-dependent NPC1 ubiquitylation does not appear to serve a major role in the control of protein degradation, since cholesterol depletion caused little effect on the steady-state levels of expressed Flag-NPC1 (Fig. 1). Its effect on the steady-state levels of endogenous NPC1 was also marginal (Fig. 6). This finding agrees with the observation by Zhang et al. (Zhang et al., 2001), who found negative effects of cholesterol depletion on the NPC1 protein levels in human skin fibroblasts. Ubiquitylated proteins can be degraded either by the lysosome or by the proteasome in the cytosol. The negative effects of the lysosomal inhibitor leupeptin on ubiquitylation of NPC1 and its steady-state levels (Fig. 3) argue against a role of the lysosome in NPC1 degradation. Our findings with the proteasomal inhibitor MG132 suggest that, like HMG-CoAR, NPC1 does undergo ubiquitylation and proteasomal degradation, but these events appear to be independent to cellular cholesterol levels. MG132 caused accumulation of ubiquitylated Flag-NPC1 and increased its steady-state levels regardless of cellular cholesterol levels (Fig. 3). MG132 induced ubiquitylation of the P691S and δLLNF mutant proteins that failed to respond to cholesterol depletion (Fig. 2). Therefore, as for the role of the proteasome in NPC1 degradation, we hypothesize that NPC1 undergoes ubiquitylation and proteasomal degradation because of protein misfolding, but not because of cholesterol depletion, and that the quality control takes place in the ER, but not in the endosome.

Our findings on the interaction between NPC1 and SKD1 suggest that ubiquitylation of NPC1 induced by cholesterol depletion serves as a sorting signal. The interaction between NPC1 and the ATP-bound, membrane-associated form of SKD1 was indicated by co-localization and co-precipitation of NPC1 and SKD1(E235Q) (Fig. 4C-E). This interaction only occurs with the ATP-bound form of SKD1, as shown by the in vitro binding of NPC1 to immobilized SKD1, which depended on the presence of ATP/ATPγs (Fig. 4F). Importantly, cholesterol depletion induced an interaction between NPC1 and wt SKD1, which presumably was in the ATP-bound, membrane-associated form (Fig. 5). The effect of cholesterol depletion on NPC1 ubiquitylation was also demonstrated for the endogenous protein in human skin fibroblasts (Fig. 6B) and, again, this ubiquitylation was accompanied by recruitment of SKD1 to the endosomal fractions (Fig. 6C). In yeast, Vps4 is required for disassembly of the ESCRT-III, which contains other Vps proteins Vps2, Vps20, Vps24 and Vps32/Snf7 (Babst et al., 2002a). Mammalian counterparts to these proteins have recently been identified (Fujita et al., 2004; Peck et al., 2004; Yan et al., 2005). Our findings suggest that NPC1 interacted with these proteins in the presence of SKD1(E235Q) or in cells depleted of cholesterol.

Two lines of questions can be addressed regarding the interaction between NPC1 and the ESCRT complex. First, how is ubiquitylated NPC1 recognized by the ESCRT complex?

Tsg101 is a mammalian ortholog of yeast Vps23 and has been shown to bind directly to ubiquitylated EGFR (Bishop and Woodman, 2001; Bishop et al., 2002). We tested whether Flag-NPC1 interacted with endogenous Tsg101 in COS cells, but could not detect any interaction between these two proteins. Therefore, it is likely that NPC1 is recognized by the ESCRT complex in a manner that is different to EGFR. Second, what is the role of the ESCRT complex in the intracellular sorting of NPC1? NPC1 is primarily localized on the late endosome and can transiently associate with cholesterol-enriched lysosomes (Higgins et al., 1999). The ESCRT complex plays a crucial role in the sorting of ubiquitylated proteins form the endosome to the lysosome through multivesicular bodies (Bishop and Woodman, 2000; Yoshimori et al., 2000; Bishop et al., 2002; Fujita et al., 2003) and, in Vps mutant yeast cells, Ncr1 is trapped in the pre-vacuolar compartments (Zhang et al., 2004), which correspond to mammalian endosomes. Therefore, it is likely that the ESCRT complex is required for the sorting of NPC1 from the late endosome to the lysosome. At least in yeast, it has been shown that the entry of the ubiquitylated protein to multivesicular bodies is preceded by de-ubiquitylation of the protein (Babst et al., 2002a). Given the effects of cholesterol depletion, we propose that the sorting of NPC1 is regulated by the local cholesterol content of the endosomal membrane. When it is low, NPC1 is ubiquitylated and is associated with the ESCRT complex. Its entry into multivesicular bodies and subsequent delivery to the lysosome might be triggered by cholesterol feeding, which presumably induces de-ubiquitylation of the protein. This sorting might be an obligatory step for the NPC1 function to relocate LDL-derived lysosomal cholesterol; further analysis is required to test our hypothesis.

Finally, our findings regarding the NPC2 cells provided an important insight into a functional relationship between NPC1 and NPC2. In cells that lack functional NPC2, ubiquitylation of NPC1 (Fig. 6B) and endosomal recruitment of SKD1 (Fig. 6C) occurred under cholesterol-rich conditions, similar to the results obtained in control cells depleted of cholesterol. Thus, under cholesterol-rich conditions, the presence of functional NPC2 was required to prevent NPC1 ubiquitylation and subsequent association with SKD1. NPC2 contains an MD-2-like lipid-recognition domain and binds cholesterol. By analogy to other proteins that contain this domain, it can be postulated that NPC2 extracts membrane-embedded cholesterol and makes it available to other proteins (Inohara and Nunez, 2002). Therefore, one possible explanation for NPC1 ubiquitylation in NPC2 cells is that cholesterol is unavailable to the membrane domains where NPC1 resides, inducing NPC1 modification that normally takes place under conditions of cholesterol deprivation. This explanation is consistent with the increased protein levels of NPC1 in NPC2 cells (Millat et al., 2001a), given that NPC1 ubiquitylation caused by cholesterol depletion does not lead to its degradation. Alternatively, it is also possible that NPC2 deficiency acts indirectly, by inducing aberrant compartmentalization of NPC1, and triggering its ubiquitylation. However, this alternative explanation does not agree with our observation that U18666A, which induces aberrant compartmentalization of NPC1, failed to affect its ubiquitylation (Fig. 1F). We suggest that cholesterol-level-dependent ubiquitylation of NPC1 is a crucial event not only to understand the intracellular sorting of NPC1 but also to unravel the functional relationship between NPC1 and NPC2 in future studies.

Materials and Methods

Materials

Dulbecco's modified Eagle's medium (DMEM), Ham's F12 medium and LipofectAMINE reagent were from Life Technologies. Bovine calf serum (BCS) was from Atlanta Biologicals. Bovine lipoprotein-deficient serum (LPDS), human LDL, anti-Flag M2 agarose and rabbit polyclonal anti-Flag antibody were from Sigma. Rabbit polyclonal anti-NPC1 antibody and mouse monoclonal antibodies against ubiquitin (P4D1), myc, His_6 and GFP were from Santa Cruz Biotech. Rabbit polyclonal anti-SKD1 has been described (Yoshimori et al., 2000).

Mammalian expression of recombinant proteins

pASC9/Flag-NPC1, an expression plasmid for human NPC1 with a Flag tag inserted in the *ClaI* site, has been described (Davies and Ioannou, 2000). pSV-SPORT/NPC1 wild-type (wt) and the P691S mutant were a gift from J. F. Strauss III (Department of Obstetrics and Gynecology, University of Pennsylvania School of Medicine, VA). The *PsyI* fragment of the Flag-NPC1 cDNA that flanks the Flag epitope was introduced to the corresponding site of pSV-SPORT/NPC1 wt and P691S to generate a Flag-tagged version of the cDNAs. The C-terminal 12 bp were deleted from pSV-SPORT/Flag-NPC1 by PCR-based mutagenesis to generate a cDNA that encoded Flag-NPC1(δLLNF). An expression plasmid for myc/His_6-tagged yeast ubiquitin was a gift from R. Kopito (Department of Biological sciences, Stanford University, CA). Expression plasmids for GFP-tagged mouse wt and E235Q mutant SKD1 have been described (Yoshimori et al., 2000). The entire coding sequence of human SKD1 cDNA (Vps4-B) (Scheuring et al., 2001) was obtained by RT-PCR with primers 5′-TCCGCCATGTCATCCACTTCG-3′ and 5′-GCTTTTGGCTTAG-CCTTCTTG-3′ from human skin fibroblasts cDNA. A His_6 epitope was introduced at the C-terminus by PCR and the cDNA was subcloned to the *EcoRI*/*XhoI* site of a mammalian expression vector pME18sf. An amino acid substitution E235Q was introduced to pME/His_6-SKD1 using a Quick Change Site-Directed mutagenesis kit (Stratagene) and was confirmed by direct sequencing. Cells were transfected using LipofectAMINE reagent according to the manufacturer's instructions.

Cell culture

COS cells and human skin fibroblasts were maintained in DMEM/10% BCS at 37°C in a humidified atmosphere containing 5% CO_2. Human skin fibroblasts were from a control human subject (H34), and from patients with NPC1 (UCH) (Yamamoto et al., 2000) and NPC2 (90031 and 88082) (Millat et al., 2001b) diseases. CHO cells were maintained in F12 medium as above. To deplete cellular cholesterol, cells were cultured for the time indicated in 10% LPDS supplemented with an HMG-CoAR inhibitor compactin (2 μM) and sodium mevalonate (0.1 mM), which assures cell viability (Ravid et al., 2000). Where indicated, this cholesterol-depleted medium was supplemented with 20 μg/ml LDL. For determination of cholesterol levels, cells in 6-well plates were scraped into PBS and lysed by sonication. Concentrations of protein and total cholesterol in the lysates were determined by using the microprotein assay kit (BioRad) and the Amplex red cholesterol assay kit (Molecular Probes), respectively, according to the manufacturer's instructions.

Immunoprecipitation and affinity purification

All procedures were carried out at 4°C. Cells were washed with PBS and lysed by sonication in buffer A [Tris-HCl 10 mM pH 7.4, NaCl 150 mM, 1 mM EDTA, 1 mM EGTA, 0.5% CHAPS and a protease inhibitor cocktail (Boehringer)]. After a brief centrifugation to remove insoluble material, the supernatant was precleared with an aliquot of agarose beads. For immunoprecipitation of Flag-NPC1, the extracts were incubated for 16 hours with anti-Flag M2 agarose beads, washed with buffer A, followed by elution of bound proteins by heating at 65°C for 10 minutes in SDS-PAGE sample buffer. SDS-PAGE, western transfer and immunoblotting were carried out as previously described (Sugimoto et al., 2001). The blot was developed using an ECL kit (Amersham Pharmacia). For immunoprecipitation of ubiquitylated proteins, cell extracts were incubated with anti-ubiquitin P4D1 antibodies for 16 hours and the immunoprecipitates were collected with protein A sepharose. For affinity purification of His_6-tagged proteins (myc/His_6-ubiquitin or His_6-SKD1), cell extracts were incubated for 16 hours with TALON metal affinity resin (Clontech). Bound proteins were analyzed as described above.

Cell fractionation

Cells were harvested in Tris-buffered saline (TBS; Tris-HCl 10 mM pH 7.4, NaCl 150 mM) supplemented with a protease inhibitor cocktail and lysed by sonication. The cell lysates were incubated on ice for 30 minutes in TBS supplemented with 1% Triton X-100 and 0.1% SDS to give total extracts. To prepare 1% Triton X-100-soluble and Triton X-100-insoluble fractions, the cell lysates were incubated in TBS + 1% Triton X-100 and, after centrifugation at 100,000 *g* for 30 minutes, the pellet was suspended in TBS + 1% Triton X-100 + 0.1% SDS. For subcellular fractionation, membranes were fractionated by using an Opti-prep gradient (Axis-

Shield) as described (Lin et al., 2004). Briefly, cells were homogenized with a potter homogenizer in ice-cold buffer (Hepes 10 mM pH 7.0, 1 mM EDTA, 1 mM EGTA supplemented with a protease inhibitor cocktail). After centrifugation at 100,000 *g* for 1 hour at 4°C, the supernatant was discarded and the pellet was resuspended in the same buffer, overlaid onto an Opti-prep gradient and centrifuged at 100,000 *g* for 16 hours at 4°C. The top 12 fractions of the gradient were recovered and numbered accordingly.

Immunofluorescence

All procedures were carried out at room temperature. Cells were fixed for 2 minutes with acetone:methanol (1:1 v/v) and incubated for 30 minutes in PBS + 1% bovine serum albumin (BSA). They were then incubated for 1 hour with anti-Flag antibody or anti-His_6 antibody in PBS + 1% BSA. Bound antibodies were visualized with an Alexa Fluor 546-conjugated secondary antibody and images were obtained using a BioRad MRC1024 confocal laser-scanning microscope.

Bacterial expression of GST-SKD1 and in vitro binding assays

The *Eco*RI/*Xho*I fragment of pME/SKD1 was transferred to pGEX-6P (Amersham Pharmacia). DH5α competent cells were transformed with the plasmid and protein expression was induced with 1 mM IPTG at 37°C for 3 hours. GST-SKD1 was recovered from bacterial pellets in 8 M urea, dialyzed against TBS and immobilized on glutathione sepharose. For in vitro binding assays, GST-SKD1 glutathione sepharose was incubated with 0.5% CHAPS extracts from Flag-NPC1-expressing cells at 4°C for 2 hours, in the absence or presence of ADP, ATP or ATPγs (all at 0.5 mM). The sepharose resin was washed with TBS + 0.5% CHAPS and bound proteins were eluted with glutathione and analyzed by SDS-PAGE followed by immunoblotting with anti-Flag antibody.

We thank J. F. Strauss III for mutant NPC1 cDNAs and R. Kopito for ubiquitin cDNA. This work was supported in part by a Grant-in-Aid for Scientific Research from the Ministry of Education, Culture, Sports, Science and Technology of Japan.

References

Babst, M., Sato, T. K., Banta, L. M. and Emr, S. D. (1997). Endosomal transport function in yeast requires a novel AAA-type ATPase, Vps4p. *EMBO J.* **16**, 1820-1831.

Babst, M., Wendland, B., Estepa, E. J. and Emr, S. D. (1998). The Vps4p AAA ATPase regulates membrane association of a Vps protein complex required for normal endosome function. *EMBO J.* **17**, 2982-2993.

Babst, M., Katzmann, D. J., Estepa-Sabal, E. J., Meerloo, T. and Emr, S. D. (2002a). ESCRT-III: an endosome-associated heterooligomeric protein complex required for MVB sorting. *Dev. Cell* **3**, 271-282.

Babst, M., Katzmann, D. J., Snyder, W. B., Wendland, B. and Emr, S. D. (2002b). Endosome-associated complex, ESCRT-II, recruits transport machinery for protein sorting at the multivesicular body. *Dev. Cell* **3**, 283-289.

Berger, A. C., Hanson, P. K., Wylie Nichols, J. and Corbett, A. H. (2005). A yeast model system for functional analysis of the niemann-pick type C protein 1 homolog, ncr1p. *Traffic* **6**, 907-917.

Bishop, N. and Woodman, P. (2000). ATPase-defective mammalian VPS4 localizes to aberrant endosomes and impairs cholesterol trafficking. *Mol. Biol. Cell* **11**, 227-239.

Bishop, N. and Woodman, P. (2001). TSG101/mammalian VPS23 and mammalian VPS28 interact directly and are recruited to VPS4-induced endosomes. *J. Biol. Chem.* **276**, 11735-11742.

Bishop, N., Horman, A. and Woodman, P. (2002). Mammalian class E vps proteins recognize ubiquitin and act in the removal of endosomal protein-ubiquitin conjugates. *J. Cell Biol.* **157**, 91-101.

Carstea, E. D., Morris, J. A., Coleman, K. G., Loftus, S. K., Zhang, D., Cummings, C., Gu, J., Rosenfeld, M., Pavan, W. J., Krizman, D. B. et al. (1997). Niemann-Pick C1 disease gene: homology to mediators of cholesterol homeostasis. *Science* **277**, 228-231.

Davies, J. P. and Ioannou, Y. A. (2000). Topological analysis of Niemann-Pick C1 protein reveals that the membrane orientation of the putative sterol-sensing domain is identical to those of 3-hydroxy-3-methylglutaryl-CoA reductase and sterol regulatory element binding protein cleavage-activating protein. *J. Biol. Chem.* **275**, 24367-24374.

Davies, J. P., Chen, F. W. and Ioannou, Y. A. (2000). Transmembrane molecular pump activity of Niemann-Pick C1 protein. *Science* **290**, 2295-2298.

Fujita, H., Yamanaka, M., Imamura, K., Tanaka, Y., Nara, A., Yoshimori, T., Yokota, S. and Himeno, M. (2003). A dominant negative form of the AAA ATPase SKD1/VPS4 impairs membrane trafficking out of endosomal/lysosomal compartments: class E vps phenotype in mammalian cells. *J. Cell Sci.* **116**, 401-414.

Fujita, H., Umezuki, Y., Imamura, K., Ishikawa, D., Uchimura, S., Nara, A., Yoshimori, T., Hayashizaki, Y., Kawai, J., Ishidoh, K. et al. (2004). Mammalian class E Vps proteins, SBP1 and mVps2/CHMP2A, interact with and regulate the function of an AAA-ATPase SKD1/Vps4B. *J. Cell Sci.* **117**, 2997-3009.

Garver, W. S., Heidenreich, R. A., Erickson, R. P., Thomas, M. A. and Wilson, J. M. (2000). Localization of the murine Niemann-Pick C1 protein to two distinct intracellular compartments. *J. Lipid Res.* **41**, 673-687.

Hicke, L. (2001). A new ticket for entry into budding vesicles-ubiquitin. *Cell* **106**, 527-530.

Higaki, K., Ninomiya, H., Sugimoto, Y., Suzuki, T., Taniguchi, M., Niwa, H., Pentchev, P. G., Vanier, M. T. and Ohno, K. (2001). Isolation of NPC1-deficient Chinese hamster ovary cell mutants by gene trap mutagenesis. *J. Biochem.* **129**, 875-880.

Higgins, M. E., Davies, J. P., Chen, F. W. and Ioannou, Y. A. (1999). Niemann-Pick C1 is a late endosome-resident protein that transiently associates with lysosomes and the trans-Golgi network. *Mol. Genet. Metab.* **68**, 1-13.

Inohara, N. and Nunez, G. (2002). ML – a conserved domain involved in innate immunity and lipid metabolism. *Trends Biochem. Sci.* **27**, 219-221.

Katzmann, D. J., Babst, M. and Emr, S. D. (2001). Ubiquitin-dependent sorting into the multivesicular body pathway requires the function of a conserved endosomal protein sorting complex, ESCRT-I. *Cell* **106**, 145-155.

Ko, D. C., Gordon, M. D., Jin, J. Y. and Scott, M. P. (2001). Dynamic movements of organelles containing Niemann-Pick C1 protein: NPC1 involvement in late endocytic events. *Mol. Biol. Cell* **12**, 601-614.

Lin, H., Sugimoto, Y., Ohsaki, Y., Ninomiya, H., Oka, A., Taniguchi, M., Ida, H., Eto, Y., Ogawa, S., Matsuzaki, Y. et al. (2004). N-octyl-beta-valienamine up-regulates activity of F213I mutant beta-glucosidase in cultured cells: a potential chemical chaperone therapy for Gaucher disease. *Biochim. Biophys. Acta* **1689**, 219-228.

Millard, E. E., Gale, S. E., Dudley, N., Zhang, J., Schaffer, J. E. and Ory, D. S. (2005). The sterol-sensing domain of the Niemann-Pick C1 (NPC1) protein regulates trafficking of low density lipoprotein cholesterol. *J. Biol. Chem.* **280**, 28581-28590.

Millat, G., Marcais, C., Tomasetto, C., Chikh, K., Fensom, A. H., Harzer, K., Wenger, D. A., Ohno, K. and Vanier, M. T. (2001a). Niemann-Pick C1 disease: correlations between NPC1 mutations, levels of NPC1 protein, and phenotypes emphasize the functional significance of the putative sterol-sensing domain and of the cysteine-rich luminal loop. *Am. J. Hum. Genet.* **68**, 1373-1385.

Millat, G., Chikh, K., Naureckiene, S., Sleat, D. E., Fensom, A. H., Higaki, K., Elleder, M., Lobel, P. and Vanier, M. T. (2001b). Niemann-Pick disease type C: spectrum of HE1 mutations and genotype/phenotype correlations in the NPC2 group. *Am. J. Hum. Genet.* **69**, 1013-1021.

Naureckiene, S., Sleat, D. E., Lackland, H., Fensom, A., Vanier, M. T., Wattiaux, R., Jadot, M. and Lobel, P. (2000). Identification of HE1 as the second gene of Niemann-Pick C disease. *Science* **290**, 2298-2301.

Patterson, M. C., Vanier, M. T., Suzuki, K., Morris, J. A., Carstea, E. D., Neufeld, E. B., Blanchette-Mackie, E. J. and Pentchev, P. G. (2001). Niemann-Pick disease type C: a lipid trafficking disorder. In *The Metabolic and Molecular Bases of Inherited Disease* (ed. C. R. Scriver, A. L. Beaudet, W. S. Sly, D. Valle, B. Childs, K. W. Kinzler and B. Vogelstein), pp. 3611-3634. New York: McGraw Hill.

Peck, J. W., Bowden, E. T. and Burbelo, P. D. (2004). Structure and function of human Vps20 and Snf7 proteins. *Biochem. J.* **377**, 693-700.

Ravid, T., Doolman, R., Avner, R., Harats, D. and Roitelman, J. (2000). The ubiquitin-proteasome pathway mediates the regulated degradation of mammalian 3-hydroxy-3-methylglutaryl-coenzyme A reductase. *J. Biol. Chem.* **275**, 35840-35847.

Scheuring, S., Rohricht, R. A., Schoning-Burkhardt, B., Beyer, A., Muller, S., Abts, H. F. and Kohrer, K. (2001). Mammalian cells express two VPS4 proteins both of which are involved in intracellular protein trafficking. *J. Mol. Biol.* **312**, 469-480.

Scott, C., Higgins, M. E., Davies, J. P. and Ioannou, Y. A. (2004). Targeting of NPC1 to late endosomes involves multiple signals, including one residing within the putative sterol-sensing domain. *J. Biol. Chem.* **279**, 48214-48223.

Sever, N., Song, B. L., Yabe, D., Goldstein, J. L., Brown, M. S. and DeBose-Boyd, R. A. (2003a). Insig-dependent ubiquitination and degradation of mammalian 3-hydroxy-3-methylglutaryl-CoA reductase stimulated by sterols and geranylgeraniol. *J. Biol. Chem.* **278**, 52479-52490.

Sever, N., Yang, T., Brown, M. S., Goldstein, J. L. and DeBose-Boyd, R. A. (2003b). Accelerated degradation of HMG CoA reductase mediated by binding of insig-1 to its sterol-sensing domain. *Mol. Cell* **11**, 25-33.

Sharma, M., Pampinella, F., Nemes, C., Benharouga, M., So, J., Du, K., Bache, K. G., Papsin, B., Zerangue, N., Stenmark, H. et al. (2004). Misfolding diverts CFTR from recycling to degradation: quality control at early endosomes. *J. Cell Biol.* **164**, 923-933.

Shenoy, S. K., McDonald, P. H., Kohout, T. A. and Lefkowitz, R. J. (2001). Regulation of receptor fate by ubiquitination of activated beta 2-adrenergic receptor and beta-arrestin. *Science* **294**, 1307-1313.

Simons, K. and Ikonen, E. (1997). Functional rafts in cell membranes. *Nature* **387**, 569-572.

Sleat, D. E., Wiseman, J. A., El-Banna, M., Price, S. M., Verot, L., Shen, M. M., Tint, G. S., Vanier, M. T., Walkley, S. U. and Lobel, P. (2004). Genetic evidence for nonredundant functional cooperativity between NPC1 and NPC2 in lipid transport. *Proc. Natl. Acad. Sci. USA* **101**, 5886-5891.

Sugimoto, Y., Ninomiya, H., Ohsaki, Y., Higaki, K., Davies, J. P., Ioannou, Y. A. and Ohno, K. (2001). Accumulation of cholera toxin and GM1 ganglioside in the early endosome of Niemann-Pick C1-deficient cells. *Proc. Natl. Acad. Sci. USA* **98**, 12391-12396.

Vanier, M. T. and Millat, G. (2004). Structure and function of the NPC2 protein. *Biochim. Biophys. Acta* **1685**, 14-21.

Watari, H., Blanchette-Mackie, E. J., Dwyer, N. K., Watari, M., Neufeld, E. B., Patel, S., Pentchev, P. G. and Strauss, J. F., III (1999a). Mutations in the leucine zipper motif and sterol-sensing domain inactivate the Niemann-Pick C1 glycoprotein. *J. Biol. Chem.* **274**, 21861-21866.

Watari, H., Blanchette-Mackie, E. J., Dwyer, N. K., Glick, J. M., Patel, S., Neufeld, E. B., Brady, R. O., Pentchev, P. G. and Strauss, J. F., III (1999b). Niemann-Pick

C1 protein: obligatory roles for N-terminal domains and lysosomal targeting in cholesterol mobilization. *Proc. Natl. Acad. Sci. USA* **96**, 805-810.

Yabe, D., Brown, M. S. and Goldstein, J. L. (2002). Insig-2, a second endoplasmic reticulum protein that binds SCAP and blocks export of sterol regulatory element-binding proteins. *Proc. Natl. Acad. Sci. USA* **99**, 12753-12758.

Yamamoto, T., Ninomiya, H., Matsumoto, M., Ohta, Y., Nanba, E., Tsutsumi, Y., Yamakawa, K., Millat, G., Vanier, M. T., Pentchev, P. G. et al. (2000). Genotype-phenotype relationship of Niemann-Pick disease type C: a possible correlation between clinical onset and levels of NPC1 protein in isolated skin fibroblasts. *J. Med. Genet.* **37**, 707-712.

Yan, Q., Hunt, P. R., Frelin, L., Vida, T. A., Pevsner, J. and Bean, A. J. (2005). mVps24p functions in EGF receptor sorting/trafficking from the early endosome. *Exp. Cell Res.* **304**, 265-273.

Yang, T., Espenshade, P. J., Wright, M. E., Yabe, D., Gong, Y., Aebersold, R., Goldstein, J. L. and Brown, M. S. (2002). Crucial step in cholesterol homeostasis: sterols promote binding of SCAP to INSIG-1, a membrane protein that facilitates retention of SREBPs in ER. *Cell* **110**, 489-500.

Yoshimori, T., Yamagata, F., Yamamoto, A., Mizushima, N., Kabeya, Y., Nara, A., Miwako, I., Ohashi, M., Ohsumi, M. and Ohsumi, Y. (2000). The mouse SKD1, a homologue of yeast Vps4p, is required for normal endosomal trafficking and morphology in mammalian cells. *Mol. Biol. Cell* **11**, 747-763.

Zhang, M., Dwyer, N. K., Neufeld, E. B., Love, D. C., Cooney, A., Comly, M., Patel, S., Watari, H., Strauss, J. F., III, Pentchev, P. G. et al. (2001). Sterol-modulated glycolipid sorting occurs in niemann-pick C1 late endosomes. *J. Biol. Chem.* **276**, 3417-3425.

Zhang, S., Ren, J., Li, H., Zhang, Q., Armstrong, J. S., Munn, A. L. and Yang, H. (2004). Ncr1p, the yeast ortholog of mammalian Niemann Pick C1 protein, is dispensable for endocytic transport. *Traffic* **5**, 1017-1030.

Journal of Cell Science

主なミトコンドリア脳筋症

電子伝達系異常症

杉江 秀夫　杉江 陽子

ミトコンドリア電子伝達系

ミトコンドリアは細胞内に存在する小器官で，嫌気性解糖の段階で1モルのグルコースから2モルのATPが産生されるのに対し，ミトコンドリア電子伝達系では36モルのATPが産生され，生体で必要なエネルギーの必要量の大部分の産生を担っている．ミトコンドリア内膜に局在している電子伝達系は，電子を内膜に伝達させて，水素イオン(H^+)をintermembrane space(膜間腔)に輸送し(電子伝達系)，生じるH^+濃度勾配(電位差，pH差)を用いて，最終段階で共役的にATPの合成を行う(酸化的リン酸化)．これらの過程をミトコンドリア呼吸鎖 mitochondrial respiratory chainと呼ぶ[1,2]．図1にミトコンドリア呼吸鎖の構成を示す．ミトコンドリア呼吸鎖は，複合体I(NADH-ubiquinone oxidoreductase)，II(SDH-ubiquinone oxidoreductase)，III(ubiquinone-cytochrome *c* oxidoreductase)，IV(cytochrome *c* oxidase：COX)と呼ばれる4つの複合体蛋白から構成され，ミトコンドリア内膜に局在している．最終的にATP合成酵素(複合体V)でATPの合成が行われる．ミトコンドリア呼吸鎖のI-Vの複合体の他にさらに3つの蛋白が電子伝達には必要である．それらはdihydroorotate-CoQ oxidoreductase(DHO-QO)，electron transfer flavoprotein-CoQ oxidoreductase(ETF-QO)，adenosine nucleotide translocator(ANT)である(表1)．ミトコンドリアの内膜にはその他coenzyme Q(CoQ，ユビキノン)，チトクローム *c* があり，CoQは内膜内を自由に動きまわり，電子を伝達したりH^+を膜間腔に汲み出す働きをしている．哺乳類では，ATPの80～90%は，ミトコンドリアでの酸化的リン酸化により生成されるが，一方ミトコンドリアはATPを合成して細胞の生を維持するだけでなく，アポトーシスにも関与し細胞の維持に

すぎえ ひでお　浜松市発達医療総合センター所長/小児神経科
すぎえ ようこ　浜松市発達医療総合センター/小児神経科

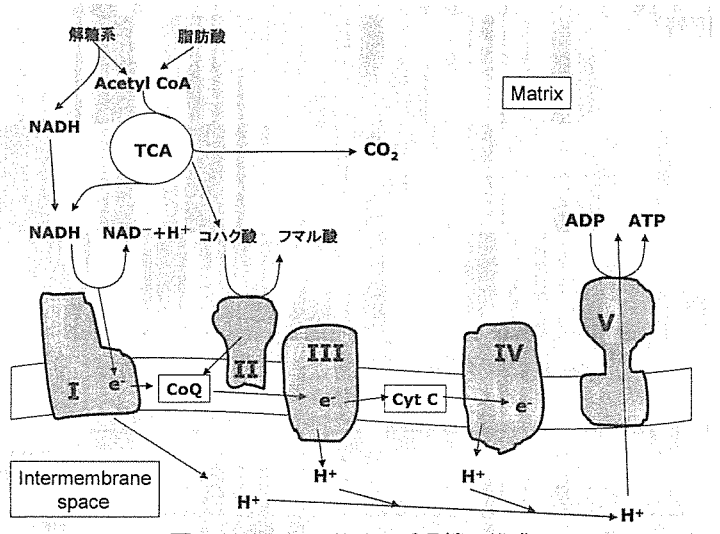

図1　ミトコンドリア呼吸鎖の構成

表1　ミトコンドリア呼吸鎖の構成

	複合体I	複合体II	複合体III	複合体IV	複合体V	DHO-QO	ETF-QO	ANT
酵　素	NADH-ubiquinone oxidoreductase	SDH-ubiquinone oxidoreductase	Ubiquinone-cytochrome *c* oxidoreductase	Cytochrome *c* oxidase	ATP synthase	Dihydroorotate-CoQ oxidoreductase	Electron transfer flavoprotein-CoQ oxidoreductase	Adenosine nucleotide translocator
サブユニット								
nDNA	43	4	10	10	14	1	1	1
mtDNA	7	0	1	3	2	0	0	0

0289-0585/06/¥500/論文/JCLS

大きな役割を果たしている.

複合体と遺伝子

複合体は表1に示すように複合体IIを除き，ミトコンドリアDNA(mtDNA)と核DNA(nDNA)の両者にコードされる複数のサブユニットから構成されている．従ってミトコンドリア病の遺伝は，mtDNAの異常に起因すれば母系遺伝を示すが，nDNAの異常であればMendel遺伝形式をとる．しかしmtDNAの巨大欠失によるものはほとんどが孤発例である．また最近父親由来のmtDNAが遺伝している例も報告され[3]，今後さらにその点の解明が必要である．一般的な臨床の場面では，pedigreeで男女ともに罹患し，母親から疾患が経由している家系ではミトコンドリア病，特にmtDNAの点変異が疑われる[4]．

筋生検と複合体の検索

一般的にミトコンドリア病はmultisystemicな症状を呈するが，脳，筋，心筋はその中でも障害を受けやすい臓器である．そのため原因検索には筋生検を用いて，組織化学，電顕，生化学検査が行われることが多い．ragged-red fiber (RRF)(図2)は筋組織化学的にミトコンドリア異常の重要な目安で，ミトコンドリア異常症の70〜80%にみられる．しかしすべてのミトコンドリア異常症に認められる変化ではない．特にnDNAの変異によると考えられる疾患ではRRFはほとんど出現しない．電子伝達系疾患の診断では生体試料として骨格筋，線維芽細胞，リンパ球などで複合体酵素活性が測定される．複合体の酵素は解糖系の酵素と異なり，酵素活性が筋の保存状態に左右され不安定であり，また病気の進行や加齢などによっても二次的に低値を示す例があるので，活性値を論ずるには様々な条件について考慮しながら解釈することが必要である[5]．一般に，複合体I＋III，II＋IIIでの活性低下がみられた場合はCoQの異常，また複合体I，II，III，およびaconitaseのすべてが低下している場合はiron sulfur proteinの異常，複合体I，II，III，IVすべての異常であれば核成分のミトコンドリアへの移送障害，またはmtDNAの欠乏，複合体I，IV欠損であればmtDNAの点変異，欠失などを疑うことができる[6]．

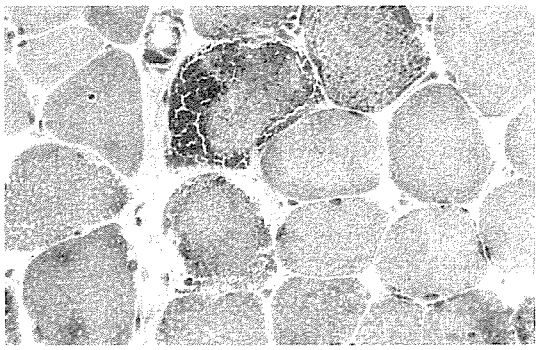

図2　MELAS患者における ragged-red fiber
Gomori-トリクローム染色.

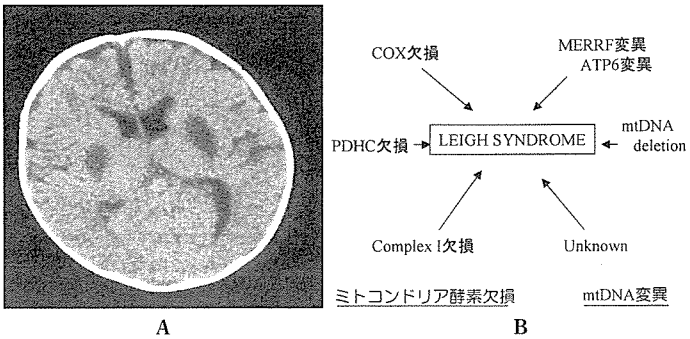

図3　Leigh脳症
A）頭部CT所見．両側基底核の低吸収が認められる．
B）原因の多様性.

複合体酵素欠損と症状の発現

ミトコンドリア病の発症頻度は約10〜15/100,000人といわれているが，症状発現には幅広いスペクトラムがあるため，実際の罹患率はもう少し多いのではないかと考えられる．またミトコンドリア病の発症には特有の病態がある．つまり，異常mtDNA(mutant mtDNA)は正常mtDNA(wild mtDNA)とさまざまな割合で細胞，臓器に分布している(heteroplasmy)ため，症状に多様性が認められる．また，発症に至るには，異常ミトコンドリアがどの程度の比率でその細胞，臓器に存在しているのかが重要で，異常mtDNAの占める比率がある閾値を超えた場合に発症につながると考えられる(threshold effect)．したがって異常ミトコンドリアを有していても閾値以下であれば無症状であったり，軽症であったりと症状の軽重，性質は広いスペクトラムを呈することとなる．ミトコンドリアはubiquitousに存在しているが，ある臓器に特異的に異常ミトコンドリアが偏在する(skewed heteroplasmy)[7]場合があり，臓器特異的な症状を示すこととなる．

ミトコンドリア病のもう一つの特徴として，異なる遺伝子異常でありながら同一の疾患の病像を呈したり，一つの遺伝子異常でありながら，示す病像が多様であったりする．

表 2　mtDNA・nDNA と主な呼吸鎖複合体(DiMauro ら[1]より)

ミトコンドリア DNA			核 DNA		
遺伝子変異	臨床像	低下を認める主な呼吸鎖酵素活性	遺伝子変異	臨床像	低下を認める主な呼吸鎖酵素活性
Single deletions	KSS	I, III, IV	*NDUF* genes*	LS	I
	PEO	I, III, IV		Leukodystrophy	I
	PS			Encephalomyopathy	I
tRNA mutations	MELAS	I, III, IV	*SDH* genes*	LS	II
	MERRF	I, III, IV		Paraganglioma	II
	Multisystemic	I, III, IV		Pheochromocytoma	II
	Myopathy	I, III, IV	*BCS I L*	LS	III
ND genes*	LHON	I		GRACILE syndrome	III
	MELAS	I	*COX* genes	Infantile myopathy	IV
	LS	I	*SURF I*	LS	IV
	Myopathy	I	*SCO* genes	Hepatopathy	IV
	Dystonia	I		Cardioencephalomyopathy	IV
*Cyt b**	Encephalomyopathy	III		Leukodystrophy	IV
	LHON	III		/tubulopathy	IV
	Myopathy	III			
	Septo-optic dysplasia	III			
	Cardiomyopathy	III			
COX genes*	LS	IV			
	Anemia	IV			
	Myopathy	IV			
	Encephalomyopathy	IV			
	ALS-like syndrome	IV			
ATPase 6 genes*	NARP	V			
	MILS	V			
	FBSN	V			

＊印は複合体サブユニットをコードする遺伝子

KSS：Kearns-Sayre syndrome, PEO：progressive external ophthalmoplegia, PS：Pearson syndrome, MELAS：mitochondrial encephalomyopathy, lactic acidosis, stroke-like episode, MERRF myoclonus epilepsy and ragged-red fiber, *ND*：NADH dehydrogenase, LHON：Leber hereditary optic neuropathy, LS：Leigh syndrome, *COX*：cytochrome *c* oxidase, NARP：neuropathy, ataxia, retinitis pigmentosa, MILS：maternally inherited Leigh syndrome, FBSN：familial bilateral striatal necrosis, *NDUF*：NADH dehydrogenase ubiquinone oxidoreductase, *SDH*：succinate dehydrogenase, GRACILE：growth retardation, aminoaciduria, lactic acidosis, and early death.

例えば Leigh syndrome(LS)は両側の基底核，脳幹，小脳などに神経画像上異常が認められ，高乳酸血症を伴う進行性の疾患であるが，病因として heterogenous な原因が報告されている(図 3 A，B)．

電子伝達系異常症は各複合体酵素活性のそれぞれの欠損を基にした生化学的分類にそって説明をされる場合が多いが，後で述べるようにそれぞれの複合体の障害で単一の疾患のみを説明できるものではなく，また複数の複合体の欠損もあり，一次的なものか，二次的なものかなど病態は複雑である．今回は複合体ごとに疾患を述べるより，遺伝子の観点と複合体酵素の生化学的な観点をあわせて述べることとする．なお各疾患についての詳細は他稿での記述を参考にしていただきたい．

遺伝子異常とミトコンドリア電子伝達系疾患(表 2)[8]

表 2 に主な遺伝子異常と複合体酵素，疾患の関係についてまとめた．

▣ mtDNA の異常に基づく電子伝達系異常症

mtDNA の異常に基づく複合体酵素活性の障害と疾患は 1 対 1 の対応ではなく，複数の複合体が障害される場合が多い．mtDNA の deletion では疾患として KSS, PEO が報告されているが，複合体酵素の異常は複数(主に I，III, IV)に異常を来す場合が多い．またミトコンドリア蛋白合成に関わる tRNA の変異では，疾患として MELAS(A 3243 G[9]など)，MERRF(A 8344 G[10]など)が有名であり，やはり複数の複合体(主に I，III，IV)の障害をおこす．ミトコンドリア複合体サブユニットをコードする遺伝子群の異常では広範な臨床症状が認められる．複合体 I の *ND* 遺伝子では MELAS，LHON，LS，複合体II の *cytochrome b* 遺伝子では運動不耐性ミオパチー[11](運動誘発による筋症状)，LHON, encephalomyopathy などがみられる．複合体IVの *COX* 遺伝子では比較的多彩な症候を示す．複合体 V では NARP，MILS，FBSN が報告されている[3]．

▣ nDNAの異常に基づく電子伝達系異常症[12]

ミトコンドリア呼吸鎖複合体をコードする遺伝子の大部分(約80遺伝子)がnDNAであることは，今後さらにnDNA遺伝子に起因するミトコンドリア病が判明してくる可能性を示唆している．また複合体サブユニットをコードしている遺伝子以外で，サブユニットのassembly, insertionに関与する蛋白などが約60遺伝子あり，複合体活性に関わっている．複合体のサブユニットをコードするnDNAの異常で発症するミトコンドリア病は複合体I，IIにのみにみられる．複合体Iの*NDUF*遺伝子異常ではLS, leukodystrophy, encephalomyopathyが，複合体IIの*SDH*遺伝子異常ではLS, paraganglioma, pheochromocytomaなどの報告がある．他に複合体のサブユニットのassemblyやinsertに関わっている核遺伝子でミトコンドリア病を呈するものは*SURF1*遺伝子で，その遺伝子異常は複合体IVの低下と臨床症状としてLSが報告されている[13]．*SCO2*，*COX15*はcardioencephalomyopathyに，*COX10*，*SCO1*はそれぞれ腎臓，肝臓を障害する．その他ミトコンドリア内に存在するnDNAにコードされる蛋白でミトコンドリア病がおこることが判明してきている．ophthalmoplegiaを示す症例や，ミトコンドリア多重欠失，mtDNA欠乏を示す例の中に，様々なnDNA遺伝子異常が見出された．それらはthymidine phosphorylase, ANT 1, Twinkle, mitochondrial polymerase γ, thymidine kinase-2, deoxyguanosine kinaseなどである(これらは他稿を参照されたい)．ミトコンドリア複合体サブユニットをコードするnDNAで複合体III, IV, Vの遺伝子異常による疾患が見出されないのは，おそらくその欠損は致死的になるためではないかと考えられている[14]．

▣ 今後の展開

ミトコンドリア電子伝達系は複雑な遺伝子のコントロール下で機能している．今後より詳細に検討がなされることにより，疾患の病態生理が判明し，またミトコンドリア病自体の分類も再編成されると思われる．

文　献

1) DiMauro S, Bonilla E. Mitochondrial encephalomyopathies. In : Engel AG, Franzini-Armstrong C, editors. Myology. New York : McGraw-Hill ; 2004. p. 1623-62.
2) Murray RK, 他. 呼吸鎖と酸化的リン酸化(14章). 上代淑人, 監訳. ハーパー・生化学(原書25版). 丸善 ; 2001. p. 149-61.
3) Schwartz M, Vissing J. Paternal inheritance of mitochondrial DNA. N Engl J Med. 2002 ; 347 : 576-80.
4) DiMauro S, Davidzon G. Mitochondrial DNA and disease. Ann Med. 2005 ; 37 : 222-32.
5) 埜中征哉. VI. ミトコンドリア病. 複合体I欠損症. 日本臨牀 領域別症候群シリーズNo 36. 日本臨牀社 ; 2001. p. 129-31.
6) Shoffner JM. Oxidative phosphorylation diseases. In : Scriver CR, et al, editors. The metabolic & molecular bases of inherited diseases. 8th ed. New York : McGraw-Hill ; 2001. p. 2367-432.
7) 太田成男. ミトコンドリアDNA：その特徴, 遺伝, ヘテロプラズミー, 閾値効果. 臨床検査. 2005 ; 49 : 9-15
8) Servidei S. Mitochondrial encephalomyopathies : gene mutation. Neuromuscul Disord. 2000 ; 10 : XVI-XXIV.
9) Goto Y. A mutation in the tRNA$^{Leu(UUR)}$ gene associated with MELAS subgroup of mitochondrial encephalomyopathies. Nature. 1990 ; 348 : 651-53.
10) Schoffner JM, Lott MT, Lezza AM, et al. Myoclonic epilepsy and ragged red fiber disease(MERRF) is associated with a mitochondrial DNA tRNA^{Lys} mutation. Cell. 1990 ; 61 : 931-7.
11) Andreu AL, Hanna G, Reichmann H, et al. Exercise intolerance due to mutations in the cytochrome b gene of mitochondrial DNA. N Engl J Med. 1999 ; 341 : 1037-44.
12) Shoubridge EA. Nuclear gene defects in respiratory chain disorders. Semin Neurol. 2001 ; 21 : 261-7.
13) Zhu Z, Yao J, Johns T, et al. SURF 1, encoding a factor involved in the biogenesis of cytochrome c oxidase, is mutated in Leigh syndrome. Nature Genet. 1998 ; 20 : 337-43.
14) DiMauro S, Schon EA. Mitochondrial respiratory-chain diseases. N Engl J Med. 2003 ; 348 : 2656-68..

主題

神経疾患

重度精神運動発達遅滞児に発症した慢性炎症性脱髄性多発根神経炎（CIDP）

石川 貴充[*1-1]・福家 辰樹[*1]
夏目 博宗[*1]・杉江 秀夫[*2]・大関 武彦[*3]

要旨

症例は多発小奇形と重度精神運動発達遅滞を基礎疾患にもつ11歳男児。約4カ月の経過で進行する上下肢の筋力低下，歩行障害を主訴に当科入院。末梢神経伝導速度は導出不能，髄液での蛋白細胞解離を認めた。臨床経過，検査所見から慢性炎症性脱髄性多発根神経炎（CIDP）と診断した。内服ステロイド治療が奏効し，臨床症状の著明な改善を認めた。本疾患は小児においては比較的稀であり，本例のように発達障害を基礎にもつ症例にCIDPが合併した場合の問題点について文献的考察を加えて報告する。

（小児科臨床　59：67，2006）

KEY WORDS ▶ chronic inflammatory demyelinating polyneuropathy（CIDP），奇形症候群，精神運動発達遅滞，ステロイド

はじめに

慢性炎症性脱髄性多発根神経（chronic inflammatory demyelinating polyneuropathy：CIDP）は1975年にDyck[1]により提唱された名称であり，慢性・再発性経過を特徴とする炎症性の末梢性脱髄性疾患である。診断には，少なくとも2カ月以上の経過で生じる一肢以上の進行性または再燃性運動感覚性末梢神経障害，そして四肢の深部腱反射の低下または消失が必須項目となる[2]。今回我々は，多発小奇形と重度精神運動発達遅滞を基礎疾患にもつCIDPの1小児例を経験したので報告する。

症　例

症例：11歳，男児

主訴：上下肢の脱力，歩行障害

既往歴：平成元年3月20日在胎38週にて出生。出生体重2,400g，新生児仮死あり。多発小奇形を認めた。8歳時に独歩可能，有意語なし。言語理解は不明であるが，声かけに対して笑顔が認められた。日常生活動作は全介助。難聴なし。現在養護学校に通学中。

家族歴：特記すべき事項なし。

現病歴：平成12年5月初旬ごろ（11歳）から歩き方がおかしい（力が入らない）様子で，約1週間前から立とうとせず，ハイハイ

＊1：榛原総合病院　小児科（〒421-0493　静岡県榛原郡榛原町細江2887-1），＊2：浜松市発達医療総合センター，＊3：浜松医科大学医学部　小児科，＊1-1：現　浜松医科大学医学部　小児科（〒431-3192　静岡県浜松市半田山1丁目20-1）

するようになったため，平成12年6月2日当科外来を受診した。その後当院の整形外科，脳神経外科も受診した。頭部 CT，脊髄 MRI を施行したが異常なし。7月14日当科を再診，7月27日に検査入院した。入院後頭部 MRI 施行するも異常を認めず，末梢運動神経伝導速度導出不能，髄液蛋白615mg/dℓと上昇を認めた。CIDP が疑われ，8月3日治療目的にて当科に再入院した。

入院時身体所見：身長131cm（−1.8SD），体重15.1kg（−2.9SD），意識清明。心肺腹部に異常所見なし。[頭部・顔面] 小頭，前額部突出，眼間開離，低い鼻梁。[四肢] 指・手・肘・足・膝関節運動制限。[筋骨格] 脊柱後側彎。独歩は不可能で起立も困難であった。

徒手筋力テストでは上腕二頭筋・三頭筋で3/5，大腿四頭筋・腓腹筋で1/5，腸腰筋・母指球筋・小指球筋は検査不能であった。深部腱反射は上・下肢とも消失，病的反射は認められなかった。

入院時検査所見：末梢血一般検査，検尿，血液生化学，血沈，免疫学的検査は，血沈軽度亢進，中性脂肪軽度上昇，尿中白血球陽性以外は異常なし。髄液検査は著明な蛋白細胞解離を呈した（**表1**）。血清中抗ガングリオシド自己抗体（GM_1，GD_{1b}，GQ_{1b}）は陰性，myelin-associated glycoprotein（MAG），sulfoglucuronosyl paragloboside（SGPG）も陰性であった。末梢神経伝導速度は，左正中神経，左腓骨神経ともに導出不能であった（**表2**）。

臨床経過：上記経過および臨床症状から，米国神経学アカデミーの診断基準[2]により，probable CIDP と診断した。8月4日よりプレドニゾロン30mg（2.0mg/kg/日），ビタミンB_{12}1,000μg/日の連日投与を開始した。投与開始5日目からズリ這いが，25日目から座位が，41日目からつかまり立ちが可能になるなど，明らかな臨床症状の改善が認められ

表1　入院時検査所見

血液一般検査				免疫学的検査	
WBC	5.8×10³/μℓ	T.Chol	185mg/dℓ	IgG	1,429mg/dℓ
RBC	4.36×10⁴/μℓ	TG	155mg/dℓ	IgA	53.8mg/dℓ
Hb	12.2g/dℓ	Na	139mEq/L	IgM	101.6mg/dℓ
Ht	36.0%	K	4.2mEq/L	抗核抗体	(−)
Plt	27.7×10⁴/μℓ	Cl	96mEq/L	抗DNA抗体	(−)
血液生化学検査		Ca	9.6mg/dℓ		
TP	7.4g/dℓ	Glucose	92mg/dℓ		
Alb	4.3g/dℓ	CRP	0.08mg/dℓ		
AST	22IU/ℓ	ESR	15.0mm/h	髄液検査	
ALT	11IU/ℓ	尿一般検査		細胞数	1/μℓ(リンパ球1)
LDH	377IU/ℓ	比重	1.015	糖	74g/dℓ
CK	151IU/ℓ	pH	7.5	Cl	120mEq/L
ALP	287IU/ℓ	蛋白	(−)	蛋白	615mg/dℓ
γGTP	11IU/ℓ	糖	(−)	IgG	42.1mg/dℓ
LAP	59IU/ℓ	ケトン体	(−)	オリゴクロナールバンド	(−)
BUN	12.0mg/dℓ	潜血	(−)	ミエリン塩基性蛋白	≦0.5ng/mℓ
Cr	0.4mg/dℓ	白血球	(2+)		
UA	4.1mg/dℓ				

表 2　運動神経伝導速度所見

Date of Exam.	Nerve	MCV (m/sec)	CMAP (mV) Dist/Prox	DL (msec)
Aug. 4,2000	Rt. Median Rt. Ulner Rt. Tibial	導出不能		
	Lt. Median Lt. Ulner LRt. Tibial	導出不能		
Sep. 7,2000	Rt. Median Rt. Ulner Rt. Tibial	14.08 3.78 6.19	0.44/0.75 1.40/1.01 0.13/0.16	39.2 31.4 63.0
	Lt. Median Lt. Ulner Lt. Tibial	6.03 3.75 8.42	0.14/0.70 0.90/0.72 0.15/0.16	29.7 29.4 48.2

た。治療開始71日目には手をつないで歩けるようになった。末梢神経伝導速度は，治療開始65日目で，低下しているものの導出可能になった（表 2）。髄液蛋白は，治療開始63日目には111mg/dℓに低下した。プレドニゾロンは投与開始36日目より漸減。経過良好にて12mg隔日投与の段階で10月18日（入院77日目）に退院した。退院後の経過も良好で，治療開始100日目には独歩可能になった。深部腱反射は，治療開始128日目ごろから認められるようになった。現在，発症以前とほぼ同等の日常生活が可能となっている。

考　察

本症例では，発症から治療開始までに約 3 カ月を要した。その理由として，患児は重度の精神運動発達遅滞を基礎にもつ発達障害児であったため，患児からの意思伝達による症状聴取が困難であり，発症当初「歩かないのか」それとも「歩けないのか」を区別することが難しかった。しかし，神経学的所見から末梢性のニューロパチーが疑われ，検査所見も含め CIDP の診断基準（“probable CIDP”）[2] を満たすニューロパチーと診断した。

本邦における CIDP の有病率は，人口10万人あたり 1～1.5と推定されており[3]，新生児，乳児を含めたあらゆる年齢層にみられると報告されている[1)4)5)]。しかしながら本邦では，15歳以下の小児について CIDP の報告は少ない[6)~19)]。これについては，1991年に米国神経学アカデミーにて CIDP の診断基準が提唱されるまでは疾患概念が不明瞭であったため，CIDP の患者が見過ごされてきた可能性が指摘されている[15]。

CIDP は運動，感覚系の末梢神経に起こる慢性進行性あるいは再発性の脱髄性多発根神経炎で，脱髄の機序は不明な点も多いが，免疫学的異常と考えられている[20]。このため本症に対しては副腎皮質ステロイド療法や免疫抑制剤の投与，免疫グロブリン大量投与など，免疫状態の適正化が治療法として試みられている。本症例では副腎皮質ステロイドが奏効し，ステロイド減量中に症状の再発は認められなかった。報告されている小児の治療例については，15症例中ステロイド（パルス療法を含む）療法が10例，γグロブリン療法が 2 例，血漿交換療法が 1 例，自然軽快が 1 例であり，ステロイド療法を選択した症例が多かった（表 3）。γグロブリン療法，血漿交換療法の症例についても当初はステロイド

表3　本邦における CIDP の報告例

報告者	報告年度	性	発症年齢	基礎疾患	治療内容	ステロイド反応性	MAG	SGPG	GM 1	GD 1 b
須貝ら	1986	男	2歳	なし	プレドニゾロン	有	——	——	——	——
目崎ら	1988	女	14歳	なし	血漿交換療法	無	——	——	——	——
酒井ら	1989	女	12歳	——	プレドニゾロン	有	——	——	——	——
松岡ら	1989	男	11歳	なし	プレドニゾロン	有	——	——	——	——
山本ら	1989	女	12歳	——	なし(自然軽快)	無	——	——	——	——
熊沢ら	1989	男	13歳	——	——	——	——	——	——	——
Takuら	1990	女	8歳	なし	γグロブリン	無	——	——	——	——
馬場ら	1992	男	12歳	遺伝性運動ニューロパチー	γグロブリン	無	——	——	——	——
若井ら	1992	女	13歳	——	プレドニゾロン	有	——	——	——	——
渡辺ら	1993	女	11歳	なし	プレドニゾロン	有	——	——	陰性	陰性
小林ら	1993	男	11歳	なし	プレドニゾロン	有	——	——	——	——
小林ら	1993	女	5歳	——	プレドニゾロン	有	——	——	——	——
青戸ら	1997	女	8歳	——	プレドニゾロン	有	×800	——	——	——
青戸ら	1997	男	7歳	——	プレドニゾロン	有	——	——	——	——
青戸ら	1997	女	12歳	——	プレドニゾロン	有	——	——	0.228	0.207
本症例	2002	男	11歳	重度精神運動発達遅滞	プレドニゾロン	有	陰性	陰性	陰性	陰性

注 ——：報告なし

療法が選択されている。このように小児 CIDP の治療について，現時点では副腎皮質ステロイド療法が主体となっている。しかし，CIDP は病状も経過も症例ごとに様々で，各治療法の効果も完全とはいえず，副作用，費用の問題もあることから，症例ごとに適切な治療法の選択が必要であろう。

近年，脱髄性末梢神経疾患において，髄鞘に対する抗体が各種検出され，病態解明の手掛かりとして注目されている。そのひとつに血清抗 GM_1 抗体がある。末梢神経の髄鞘は，主に蛋白質と脂質から構成されている。脂質の主体性分であるガングリオシドは主として GM_1 および GD_{1a} から構成されており，その GM_1 に対する抗体が M 蛋白血症にともなうニューロパチーや，運動神経障害を主体とするニューロパチーで認められることが報告されている[21)22)]。CIDP に関しては，抗 GM_1 抗体が検出された報告が散見されてはいるが，運動ニューロン疾患や多巣性運動ニューロパチー例と比べ陽性頻度は低い[23)]。本症例においても，抗 GM_1 抗体は陰性であった。

最近では，ガングリオシド抗体以外の酸性糖脂質に対する血清中の自己抗体が注目されている。ひとつは myelin-associated glycoprotein (MAG) であり，もうひとつは sulfoglucuronosyl paragloboside (SGPG) である。MAG が中枢神経系にも多量に含まれるのに対し，SGPG は末梢神経に特異的な糖脂質であり，多発神経炎患者の血中抗体の標的抗原である可能性が議論されている。SGPG は強い免疫原性を持ち，末梢神経炎の標的になり得るため，抗 SGPG 抗体陽性の症例ではステロイド治療抵抗性を呈する例もある[24)]。本症例では MAG，抗 SGPG 抗体とも陰性であり，ステロイド治療奏効との関連性も示唆された。

結　語

CIDP の11歳男児例を報告した。本症例はステロイド内服治療が奏効した。小児期発症の CIDP の報告を比較し，ステロイド反応性は本症例も含めた14例中13例（92.9%）に認められた。患児は多発小奇形と重度精神運動発達遅滞を基礎にもっており，他覚的な神経学的所見の重要性をあらためて考えさせる貴重な症例と思われた。

文　献

1) Dyck PJ et al：Chronic inflammatory demyelinating polyneuropathy. Mayo Clin Proc 50：621～637, 1975
2) Ad Hoc Subcommittee of the American Academy of Neurology AIDS Task Force：Research criteria for diagnosis of chronic inflammatory demyelinating polyneuropathy (CIDP). Neurology 41：617～618, 1991
3) 馬場正之：Chronic inflammatory demyelinating polyneuropathy －multifocal demyelinationg neuropathy－. 脳神経 44：709～718, 1992
4) McCombe PA, Pollard JD, McLeod JG：Chronic inflammatory demyelinating polyneuropathy. A clinical and electrophysiological study of 92 cases. Brain 110：1617～1630, 1987
5) Prineas JW, Mcleod JG：Chronic relapsing polyneuritis. J Neurol Sci 27：427～458, 1976
6) 若井周治：Chronic inflammatory demyelinating polyneuropathy の1女児例. 臨床小児医学 40：181～184, 1992
7) 須貝研司：慢性再発性多発神経炎. 小児科 27：1367～1379, 1986
8) 目崎高広：血漿交換療法が劇的な効果を示した慢性再発性多発神経炎. 神経内科 29：167～171, 1988
9) 酒井規雄：慢性脱髄性脳脊髄末梢神経炎. 神経内科 30：30～37, 1989
10) 松岡幸彦：Chronic inflammatory demyelinating polyneuropathy の臨床特徴. 神経内科 31：1～7, 1989
11) 山本辰紀：Chronic inflammatory demyelinating polyneuropathy における腓腹神経の組織学的所見. 神経内科 31：8～14, 1989
12) 熊沢和彦：慢性再発性・進行性多発根神経炎の自律神経障害. 臨床神経 29：994～999, 1989
13) Taku T, Tamura T, Miike T：Ganmaglobulin therapy in a case of chronic relapsing dysimmune polyneuropathy. Brain Dev 12：247～249, 1990
14) 馬場正之：小児の慢性炎症性脱髄性根神経炎（CIDP）：遺伝性ニューロパチーとの症候学的類似点とその臨床的問題点. ニューロパチーの臨床と病態に関する研究班平成3年度研究報告書, p.121～124, 1992
15) 小林由美子：慢性炎症性脱髄性根神経炎（CIDP）の1小児例. 東女医大誌 63(臨時増刊)：285～292, 1993
16) 永富文子：乳児期発症の慢性炎症性脱髄性多発ニューロパチーの1例. 日本内科学会雑誌 88：704～706, 1999
17) 織田雅也：著明な onion bulb 様の病理変化を呈し遺伝性末梢神経障害に類似した慢性再発性脱髄性多発根神経炎の若年発症例. 脳神経 51：1075～1079, 1999
18) 渡辺幸恵：慢性炎症性脱髄性多発根神経炎を合併した多発性硬化症. 脳と発達 25：70～75, 1993
19) 青戸和子：小児期発症の慢性脱髄性多発ニューロパチーの長期治療における臨床的検討. 北里医学 27：45～51, 1997
20) Dyck PJ, Prineas J, Pollard J：Chronic inflammatory demyelinating polyneuropathy. In peripheral neuropathy, 3rd de, ed by Dyck PJ, Thomas PK, Griffin JW, et al, W.B. Saunders, Philadelphia, p.1498～1571, 1993
21) Pestronk A, Chaudhry V, Feldman E L：Lower motor neuron syndromes defined by patterns of weakness, nerve conduction abnormalities, and high titers of antiglycolipid antibodies. Annals of Neurology 27：316, 1990
22) Sadiq S A, Thomas F P, Kilidireas K：The spectrum of neurologic disease associated with anti-GM1 antibodies. Neurology 40：1067, 1990
23) 西尾建資，梶　龍児：抗 GM1 ガングリオシド抗体と神経系. 診断と治療 81：715～719, 1993
24) 山脇正永，水澤英洋：硫酸化グルクロン酸含有糖脂質（SGPG）と末梢神経疾患. 脳の科学 20：1129～1134, 1998

ARTICLE doi:10.1016/j.ymthe.2005.09.020

Histopathological and Behavioral Improvement of Murine Mucopolysaccharidosis Type VII by Intracerebral Transplantation of Neural Stem Cells

Yasuyuki Fukuhara,[1,2] Xiao-Kang Li,[3] Yusuke Kitazawa,[3] Masumi Inagaki,[4] Kentaro Matsuoka,[5] Motomichi Kosuga,[1] Rika Kosaki,[1,2] Takuya Shimazaki,[6] Hitoshi Endo,[7] Akihiro Umezawa,[8] Hideyuki Okano,[6] Takao Takahashi,[2] and Torayuki Okuyama[1,2,*]

[1]*Department of Clinical Genetics and Molecular Medicine,* [3]*Department of Innovative Surgery,* [8]*Department of Reproductive Biology, and* [5]*Department of Pathology, National Center for Child Health and Development, 2-10-1 Okura, Setagaya-ku, Tokyo 157-8535, Japan*
[2]*Department of Pediatrics and* [6]*Department of Physiology, Keio University School of Medicine, 35 Shinanomachi, Shinjuku-ku, Tokyo 160-8582, Japan*
[4]*National Center of Neurology and Psychiatry, 1-7-1 Kounodai, Ichikawa-shi, Chiba 272-8516, Japan*
[7]*Biochemistry of Experimental Medicine, Jichi Medical School, Minamikawachi-machi, Kawachi-gun, Tochigi 329-0498, Japan*

**To whom correspondence and reprint requests should be addressed. Fax: +81 3 3416 2222. E-mail: okuyama-t@ncchd.go.jp.*

Available online 28 November 2005

The therapeutic efficacy of neural stem cell transplantation for central nervous system (CNS) lesions in lysosomal storage disorders was explored using a murine model of mucopolysaccharidosis type VII (MPS VII). We used fetal neural stem cells derived from embryonic mouse striata and expanded *in vitro* by neurosphere formation as the source of graft materials. We transplanted neurospheres into the lateral ventricles of newborn MPS VII mice and found that donor cells migrated far beyond the site of injection within 24 h, and some of them could reach the olfactory bulb. A quantitative measurement indicated that the GUSB activity in the brain was 12.5 to 42.3% and 5.5 to 6.3% of normal activity at 24 h and 3 weeks after transplantation. In addition, histological analysis revealed a widespread decrease in lysosomal storage in the recipient's hippocampus, cortex, and ependyma. A functional assessment with novel-object recognition tests confirmed improvements in behavioral patterns. These results suggest that intracerebral transplantation of neural stem cells is feasible for treatment of CNS lesions associated with lysosomal storage disorders.

Key Words: neurosphere, mucopolysaccharidosis type VII, intracerebral transplantation

Introduction

Mucopolysaccharidosis type VII (MPS VII), or Sly syndrome, is a congenital lysosomal storage disorder (LSD) characterized by a systemic deficiency of β-glucuronidase (GUSB) activity [1]. This defect results in a progressive accumulation of undegraded glycosaminoglycans and subsequent lysosomal distension in multiple tissues, including the central nervous system (CNS). Enzyme replacement therapy and bone marrow transplantation are effective for correcting visceral manifestations of the disorder [2,3]. However, effective treatment of the CNS in patients with LSDs remains a major challenge.

With respect to cell therapy directed to the CNS in an MPS VII mouse, there are reports that the intracerebral transplantation of a genetically engineered neural progenitor [4] and retrovirally transduced syngeneic fibroblasts [5] corrected the lysosomal storage of the recipient's brain tissues. We also previously reported that adeno virally transduced rat amniotic epithelial cells injected into adult MPSVII mouse brains survived at the injection point for more than 9 weeks and the subsequent supply of enzyme resulted in pathological improvement in multiple areas of the MPS VII mouse brains [6].

In this study, we used fetal neural stem cells derived from embryonic mouse striata and expanded *in vitro* by neurosphere formation [7,8] as the source of graft materials. Neural stem cells are considered to be good candidates for cell therapy to treat CNS dysfunction. In fact, fetal neural tissues have been successfully used in human Parkinson disease patients [9,10]; however, as many as four to eight fetuses were required to obtain a sufficient number of cells to treat a single patient. Expansion of neural stem cells *in vitro* may overcome the above practical

Abbreviations used: CNS, central nervous system; GUSB, β-glucuronidase; MPS VII, mucopolysaccharidosis type VII.

1525-0016/$30.00

and ethical problems associated with fetal tissue transplantation and provide a source for graft material.

Here we describe improvements in the histopathology of the hippocampus, cortex, and ependyma and in nonspatial hippocampus-dependent learning and memory evaluated in a novel-object recognition test at 2 months after transplantation. These data suggest that early transplantation of neurospheres into the CNS may prevent or delay some of the progressive mental impairment associated with this LSD.

Results and Discussion

Production and Secretion Capacity of GUSB Enzymes by Neurospheres

The neurosphere is a floating cell cluster containing plenty of neural stem cells and is generated from a fetal mouse brain by neurosphere formation [7,8]. Briefly, when we culture fetal corpus striatum containing neural stem cells in a serum-free medium with growth factors, only neural stem cells can survive and form floating cell clusters called neurospheres. We initially determined the endogenous GUSB activity of neurospheres obtained from normal C57BL/6 mice. The GUSB activity of the neurosphere and its culture medium proved significantly higher than that of bone marrow cells (Figs. 1A and 1B). We also evaluated the difference in GUSB activity before and after differentiation. Most neurospheres differentiate into neural cells *in vivo* according to their microenvironments after transplantation [8]. The GUSB activities in differentiated cells and their culture media were almost equivalent to those of bone marrow cells, suggesting that the GUSB activity of the neurospheres was reduced, although it was maintained to the extent necessary for a therapeutic effect even after differentiation.

Intercellular Transport of the GUSB Enzyme

It is well known that most lysosomal enzymes can be taken up into cells by M6P receptor-mediated endocytosis, and that this process is efficiently blocked in the presence of M6P [11]. When we transferred the culture medium of neurospheres generated from C57BL/6 fetal mouse brains to dishes of the primary culture of neurons generated from C3H mice, 21.9% of the heat-stable C57BL/6 mouse-derived GUSB in the culture medium was internalized into the neurons in the absence of M6P (Fig. 1C). In contrast, it was significantly reduced in the presence of 10 mM M6P (Fig. 1C). This suggests that endocytosis by M6P receptors leads to the internalization of the GUSB enzyme secreted from the neurospheres to the neurons.

Lysosomal Enzyme Activities of the Neurosphere

Many LSDs display CNS symptoms. Most lysosomal enzymes have common transport systems mediated by the M6P receptor, and therefore the same transplantation strategy could be available if neurospheres can produce and secrete significant amounts of lysosomal enzymes. We determined the specific activities of several lysosomal enzymes in neurospheres and compared them with those in marrow stromal cells and human granulocytes. Similar or higher activities of lysosomal enzymes were identified in the neurosphere (Table 1).

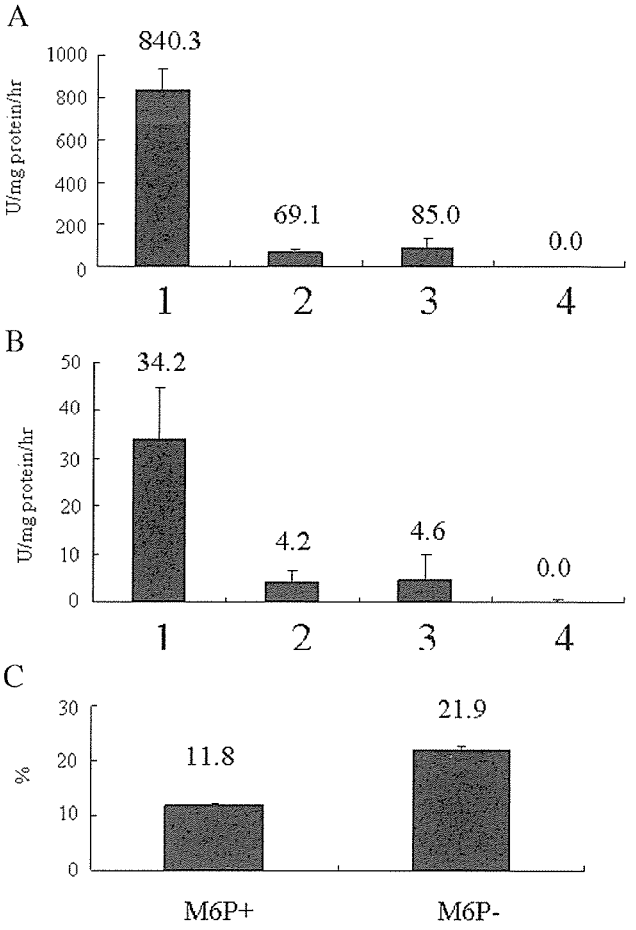

FIG. 1. Neurosphere GUSB activities and secretion via cell-to-cell transport. Lanes 1, neurospheres; 2, differentiated cells from neurospheres; 3, bone marrow cells; 4, 3521 cells (fibroblasts that originated from an MPS VII mouse). The GUSB activities of the neurosphere and its culture medium proved significantly higher than those of bone marrow cells. The GUSB activity in differentiated cells from neurospheres and that of its culture medium were almost equivalent to those of bone marrow cells. (A) GUSB activity in cell pellets of the neurosphere, bone marrow, and 3521 cells. (B) GUSB activity in a culture medium of the neurosphere, bone marrow, and 3521 cells at the time of the first passage. (C) Cell-to-cell transport of GUSB secreted from neurospheres. The ratio of the heat-stable GUSB activity in C3H mouse neural cells to the total heat-stable GUSB activity in the culture medium was calculated. The means ± standard errors are provided.

Distribution of Donor Cells after Neonatal Transplantation

We performed a syngeneic transplantation experiment using neurospheres obtained from CAG-EGFP transgenic

doi:10.1016/j.ymthe.2005.09.020

TABLE 1: Activities of lysosomal enzymes in the neurosphere and their related diseases[a]

Lysosomal enzyme	Disease	Neurosphere	MSC[b]	Granulocytes
α-L-Iduronidase	**MPS I**	**39.2**	**57.4**	**56–201 (*n* = 6)**
Iduronate sulfatase	**MPS II**	**40.5**	**20**	**12–26 (*n* = 5)**
Heparan-*N*-sulfatase	**MPS IIIA**	**1.1**	**4.3**	**0.2–3 (*n* = 4)**
GalNAc-6-*S*-sulfatase	**MPS IVA**	**5.3**	**15.2**	**8.1–20 (*n* = 5)**
Arylsulfatase B	**MPS VI**	**55.3**	**15.5**	**9–32 (*n* = 5)**
β-Glucosidase	**Gaucher disease**	**3.0**	**6.5**	**0.2–0.6 (*n* = 100)**
α-Galactosidase A	**Fabry disease**	**189**	**68.8**	**49.8–116.4 (*n* = 48)**
β-Galactosidase	**MPS IVB**	**501**	**309**	**37.6–230.1 (*n* = 100)**
α-Mannosidase	**α-Mannosidosis**	**61.0**	**48.0**	**121.1–345.1 (*n* = 100)**
β-Hexosaminidase	**Sandhoff disease**	**1024**	**3062**	**401.7–1426.0 (*n* = 100)**
β-Hexosaminidase A	**Tay–Sachs disease**	**527**	**481**	**251.1–607.4 (*n* = 48)**
Arylsulfatase A	**MLD**	**435**	**278**	**109.0–217.2 (*n* = 100)**

[a] We quantitatively assayed for a variety of lysosomal enzymes as well as GUSB. Several kinds of lysosomal enzymes were found to be high in the neurosphere. This result suggests that the neurosphere may be applied for the treatment of different types of congenital metabolic disorder. Data are given in nmol/mg protein/h. Enzyme activities in human granulocytes were measured as described elsewhere [27].
[b] MSC, marrow stromal cell.

mice (C57BL/6 background) as donor cells and newborn MPS VII mice as recipients. We injected 2.5–5 × 10^4 neurospheres (Fig. 2A) into the lateral ventricles of neonatal MPS VII mice within 1 to 3 days after delivery. A large number of donor cells were located mainly in the periventricular area at the hippocampus level in the brain, but a small number of GFP-positive cells were observed at varying distances away from the periventricular area at 24 h (Fig. 2B). We identified some of the GFP-positive cells in a linear formation at the level of the olfactory bulb, indicating a specific manner of migration in this area that is referred to as chain migration [12] (Fig. 2C). The overall distribution of the donor cells throughout the brain was essentially identical in all mice examined histologically (n = 3), with findings similar to previous reports [4,13–15]. There was evidence of GUSB

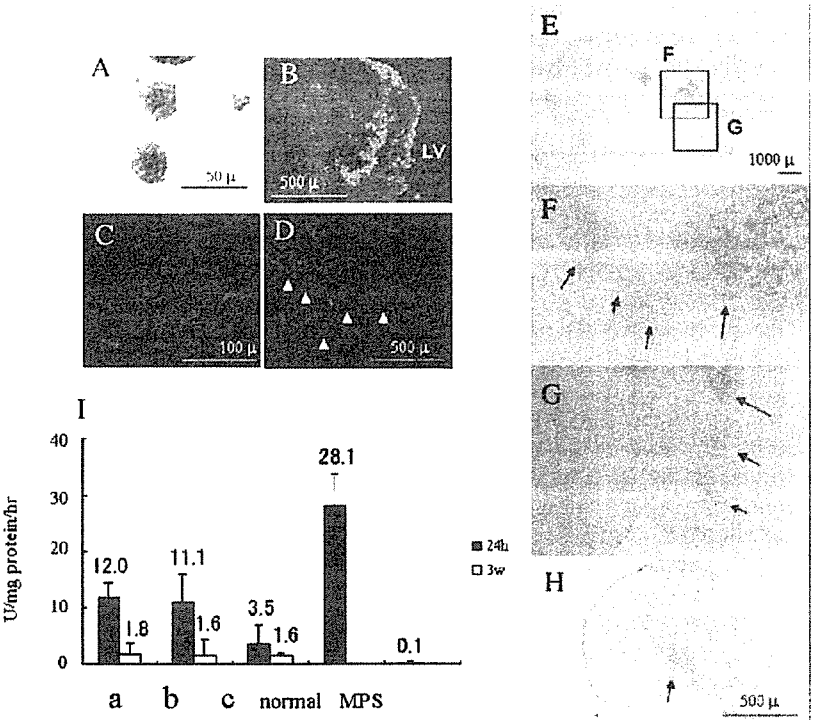

FIG. 2. Distribution of the donor cells in a mouse brain following transplantation of neurospheres. (A) Neurospheres generated from GFP transgenic mice under a fluorescence microscope. (B) A slice at the hippocampus level in the brain at 24 h after transplantation under a fluorescence microscope. GFP-positive cells were located mainly in the periventricular area. (C) A slice at the olfactory bulb level in the brain at 24 h after transplantation. GFP-positive cells were also detected under a fluorescence microscope; some of them were found to form a line (a chain migration). (D) A slice at the hippocampus level in the brain under a fluorescence microscope at 3 weeks after transplantation. GFP-positive cells were found to be branched and to form a network with the recipient brain tissue. (E–H) The brain of an MPS VII mouse at 24 h after transplantation of neurospheres. The recipient brain was stained red by GUSB staining in accordance with the GFP-positive area. (E–G) Coronal sections of the telencephalon at the caudal level. (H) Olfactory bulb. (I) Quantitative determination of the GUSB activity was performed at 24 h and 3 weeks after transplantation. The brains of the transplant recipients were divided coronally into three parts and quantitatively assayed for GUSB activity (n = 3). The regions used for evaluation at the designated times were defined by anatomical landmarks in the anterior-to-posterior plane: a, olfactory bulbs; b, caudal edge of the olfactory bulbs to the rostral edge of the hippocampus; c, hippocampus to the posterior colliculus. The cerebellum was dissected free and was not included in the assay.

staining in accordance with the GFP-positive area, indicating a rise in GUSB activity (Figs. 2E–2H).

We previously reported that neurosphere-derived donor neurons extend their processes into the host tissues and form a synaptic structure [8]. The GFP-positive cells had extended their processes and formed synaptic structures as well 3 weeks after transplantation (Fig. 2D). These data suggest that the donor cells migrated from the periventricular area and some of them reached the olfactory bulb as early as 24 h after transplantation.

Quantitative Gusb Assay in Transplanted Mouse Brains

We divided the brains of the transplant recipients coronally into three parts and quantitatively assayed them for GUSB activity at 24 h (n = 3) and 3 weeks (n = 3) after transplantation (Fig. 2I). GUSB activity was 12.5 to 42.3% of normal activity at 24 h. There was 5.5 to 6.3% of normal activity at 3 weeks after transplantation. This is an amount at which that lysosomal distensions in the neuron and glia could also be reversed [16]. These results imply that donor cells provided the recipient brain with GUSB activity to the extent that lysosomal storage in the recipient brain could be prevented for at least 3 weeks.

Histological Analysis and Tumorigenesis Assessment of the Treated Mice

We tested the treated MPS VII mice for reduction of lysosomal distensions in the neurons and glia at 2 months after transplantation (n = 2) (Figs. 3 and 4). We performed a histological analysis on hippocampus, cortex, and ependyma using an optical microscope (hippocampus, cortex, and ependyma) and an electron microscope (cortex). In the hippocampus of the untreated MPS VII mice, most of neurons contained marked cytoplasmic vacuolation (lysosomal storage) as well as astrocytes. In contrast, those of the treated hippocampuses were almost eliminated especially from neurons in this area. In the cortices, we also observed extensive neuronal and glial vacuolation, and the treatment reduced them remarkably as well. An electron microscope demonstrated that lysosomal storage in some neurons was completely eliminated in this area

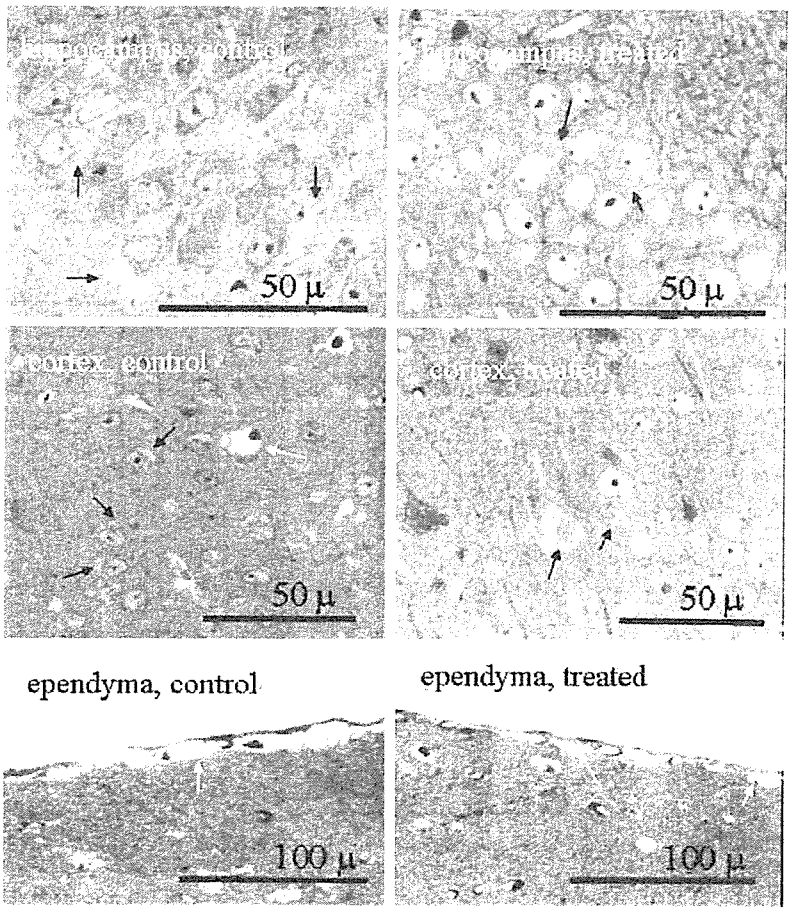

FIG. 3. Toluidine blue-stained, 0.5-μm-thick sections from the hippocampus, cortex, and ependyma are from 2-month-old MPS VII mice (n = 2). Intraventricular injection of neurospheres decreases lysosomal storage in the hippocampus, cortex, and ependyma. Black arrows indicate distended vacuoles in neurons; white arrows indicate storage in glia.

doi:10.1016/j.ymthe.2005.09.020

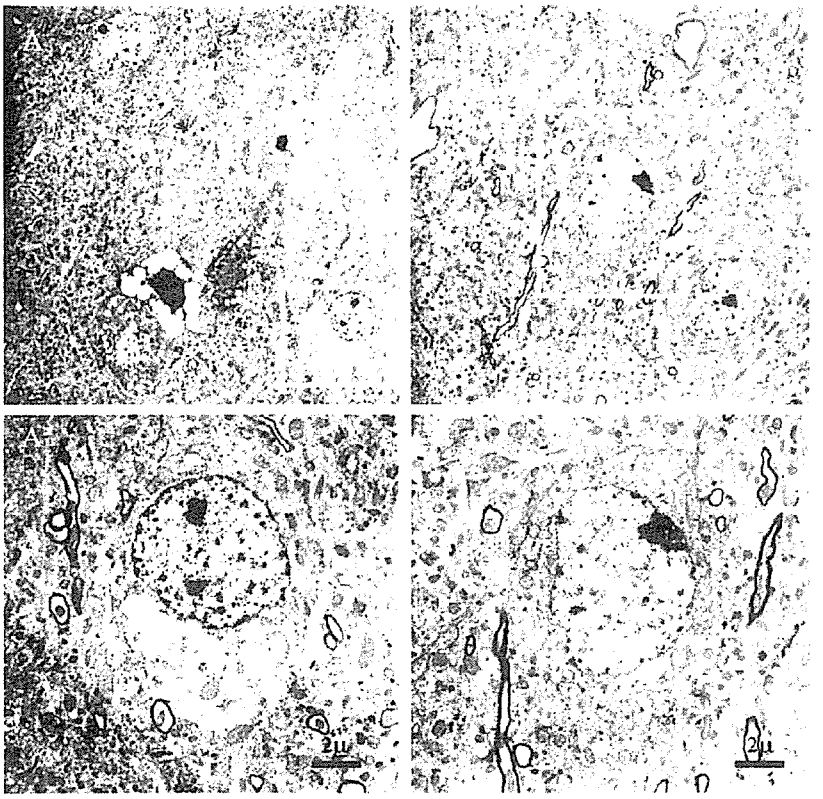

FIG. 4. Electron microscopic analysis of lysosomal storage in a mouse brain following transplantation of neurospheres. (A) Cortex of a control untreated MPS VII mouse at 2 months after transplantation. Abundant white cytoplasmic vacuoles represent distended lysosomes. (B) Cortex of a MPS VII mouse at 2 months after transplantation. Lysosomal storage granules in this area were remarkably reduced in size and number, and those in some neurons were completely eliminated. (A′ and B′) Magnified photographs of the circumscribed areas in (A) and (B).

(Fig. 4). In the ependyma, the amount of storage appeared to be significantly reduced in the treated mice. To evaluate quantitatively the improvement of the pathology in the treated mice, we counted neurons and glia containing apparent vacuolation in each hippocampus and cortex of the treated and the untreated mice ($n = 2$, total 300 cells in each area) in the HPF (×600). In both areas, we observed a remarkable decrease in the number of neurons and glia with apparent lysosomal storage, and this finding was almost equal in two treated mice, indicating an improvement of the pathology in the treated mouse brains (Table 2). We carefully assessed all transplanted mice for the presence of tumorigenesis. We dissected the brains of the dead mice during the course of the study and macroscopically analyzed them for tumor formation, but we could not identify any tumor formation among them.

TABLE 2: The percentage of cells with apparent vacuolization in the brain of MPS VII mice treated with intraventricular injection of neurospheres[a] ($n = 2$)

	Untreated	Treated
Hippocampus	**89.3%**	**17.3%**
Neuron	**90%**	**18.4%**
Glia	**92%**	**13.9%**
Cortex	**42%**	**15.3%**
Neuron	**37.7%**	**11.7%**
Glia	**55.6%**	**30%**

[a] Toluidine blue sections of hippocampus and cortex were analyzed for lysosomal distention, and we counted neurons and glia containing much vacuolation in 300 cells in each of hippocampus and cortex in the HPF (×600).

Mouse Hearing Acuity Assessment

Measurements of the auditory brain-stem response (ABR) have been useful in assessing functional improvements after treatment [17]. We tested three treated MPS VII mice, three untreated MPS VII mice, and three C57BL/6 mice. There was no significant difference in the ABR thresholds among the treated and the untreated MPS VII mice (Fig. 5A). It is well known that malalignment and focal loss of stereocilia occur as the disease progresses, leading to a sensorineural hearing loss [18]. As the ABR was performed at 2 months, it may have been too early to assess the sensorineural hearing loss.

Behavioral Assessment

We used a novel-object recognition test, a tool for studying nonspatial hippocampus-dependent memory, to determine whether an improvement in mental status could be achieved by transplantation [19–21]. We carried out this test as described [19] with several modifications at 2 months after transplantation ($n = 3$). We used normal siblings of the treated MPS VII mice as the control mice. In summary, after the mice were habituated to an open field, two yellow objects (A, B) were placed diagonally in

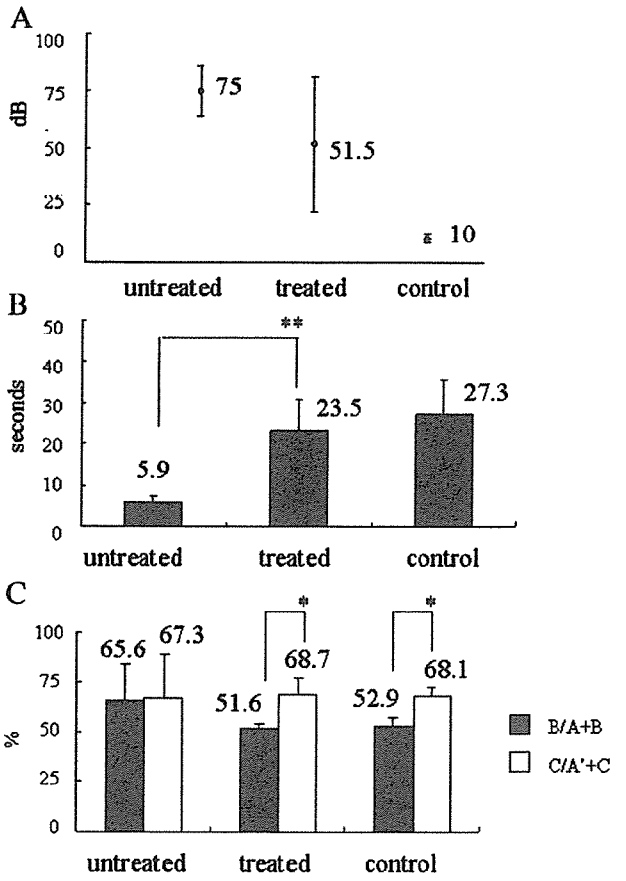

FIG. 5. Assessment of the functional recovery at 2 months after transplantation. (A) Auditory-evoked brain-stem responses. The decibels required to elicit ABR at the broadband (clicks) were evaluated among three normal mice, three treated MPS VII mice, and three untreated MPS VII mice at 2 months after transplantation. There was no significant difference in the ABR thresholds among the treated MPS VII mice and the untreated MPS VII mice. (B) The novel-object recognition test. The mice were assessed for an improvement in hippocampus-dependent nonspatial memory by a novel-object recognition test ($n = 3$). The total time spent exploring objects on day 4 (=A + B) in the treated mice was significantly longer than that for the untreated mice. (**$P < 0.01$). (C) The novel-object recognition test (retention test). The percentage of time spent in exploring B as a portion of the total object exploration time on day 4 [B/(A + B)] was compared with that of C (the novel object) on day 5 [C/(A′ + C)]. C/(A′ + C) in the C57BL/6 and the treated mice was significantly greater than B/(A + B). This suggests that the normal mice and the treated mice spent a significantly longer time exploring the novel object, revealing that both groups had a significant preference for exploring the novel object. The means ± standard errors are provided.

the open field on day 4, and the mice were allowed to explore them for 10 min. Object B was replaced with a novel object (C) and the other object was replaced with a replica (A′) on day 5, and the mice were again allowed to explore them for 10 min. Normal animals prefer to explore the novel object more than the familiar object. From the degree of preference for exploration of the new object, it can be inferred that they retained a memory of the familiar object. The total time spent exploring object A or B on day 4 (=A + B) was 27.3 ± 8.4 s in the normal mice, 23.5 ± 7.4 s in the treated mice, and 5.9 ± 1.6 s in the untreated mice (Fig. 5B), indicating that the normal and the treated mice had the same levels of motivation, curiosity, and interest in exploring objects. Next, to evaluate preferential exploration of the novel object, we compared the percentage of time spent exploring object B as a portion of the total object-exploration time on day 4 [=B/(A + B)] with that of object C (the novel object) on day 5 [=C/(A′ + C)] (Fig. 5C). C/(A′ + C) in the normal and the treated mice was significantly greater than B/(A + B) [normal mice, B/(A + B) = 52.9 ± 3.9%, C/(A′ + C) = 68.1 ± 4.4%; treated mice, B/(A + B) = 51.6 ± 2.8%, C/(A′ + C) = 68.7 ± 8.4% of the exploration time]. This indicates that the normal mice and the treated mice spent a significantly longer time exploring the novel object, revealing that both groups exhibited a significant preference for exploring it. These results indicate that the treated mice have the same level of nonspatial hippocampus-dependent memory as the normal mice. But we cannot completely deny the possibility that the vision had an influence on this improvement of a novel object test.

To date, there are reports demonstrating an improvement in behavior of treated MPS VII mice assessed by a Morris water maze test [22,23]. We used a novel-object test because it is very easy and less of a burden on the mice than the Water maze test. Consequently, it is easily applicable to mice with motility disturbance, and we thought we could maximize mouse performance associated with visual recognition memory. The long-term effects of this treatment have not been examined in detail. The treated mice lived to 7 months of age at most. Transplantation of neurospheres did not extend the life span of MPS VII mice. Life span may be dependent on systemic lysosomal storage other than the CNS.

In summary, our results demonstrated that after transplantation of *in vitro*-expanded neurospheres into the neonatal ventricle of MPS VII mice brains, the transplant donor cells migrated along established routes and integrated into the recipient's brain. The treated mice exhibited improved cognitive functions as measured by a novel-object recognition test, which was consistent with histological evidence of reduced lysosomal storage in the brain tissue.

Materials and Methods

Animals. Syngeneic MPS VII (*mps/mps*) mice were obtained from a pedigree colony of B6.C-H-2^{bm1}/ByBir-gus^{mps}/+ mice maintained at our facility [6]. Normal C3H mice were purchased from Shizuoka Laboratory Animal Center (Shizuoka, Japan). CAG-EGFP transgenic mice were originally generated by Endo *et al.* [24,25]. All mice were maintained and treated in accordance with the guidelines of the animal committee of the facility.

Isolation, primary cultures, and passaging procedures of neurospheres. Embryos were removed from CAG-EGFP transgenic mice on day 14.5 of pregnancy. The corpus striatum was dissected and prepared as described

doi:10.1016/j.ymthe.2005.09.020

elsewhere [7]. Neurospheres were cultured in the medium described below at 37 °C with 5% CO_2 at a concentration of 2×10^5 cells/ml in the primary culture. The culture medium was DMEM/F12 supplemented with the hormone mixture used by Reynolds and Weiss [7]. Passages were performed once per week. Neurospheres were used for the transplantation after the second to fifth passage.

Cell-to-cell transport of GUSB secreted from neurospheres. We evaluated *in vitro* the uptake ratio of the GUSB enzyme secreted from neurospheres of C57BL/6 mice into neural cells of C3H mice by using the difference in the heat stability of GUSB proteins between C57BL/6 mice and C3H mice. In brief, GUSB activity of C57BL/6 mice was reduced by only 30% after a 2-h incubation at 65 °C [11]. In contrast, GUSB activity of C3H mice was decreased markedly after this procedure. We prepared a culture medium of neurospheres from C57BL/6 mice after 1 week incubation. We replaced the medium of primary neurons of C3H mice with the above medium, continued to culture in the presence or absence of M6P, and harvested 12 h later. Heat-stable GUSB activity in the homogenates of C3H mouse neurons was measured after a 2-h incubation at 65 °C.

Quantitative analysis of GUSB activity. GUSB activity in tissues and cell homogenates was quantified using a fluorometric assay described previously [26]. Neurospheres were quantitatively analyzed after the second to fifth passage. Differentiated cells were obtained from neurospheres by converting the culture medium into DMEM +10% FBS. We had previously demonstrated that these cells differentiated into neurons, astrocytes, and oligodendrocytes by immunological staining (data not shown). Bone marrow was isolated from C57BL/6 mice and cultured in DMEM +10% FBS. Attached cells were collected after the second to fifth passage and analyzed for GUSB activity.

Histochemical detection of GUSB activity. The mice were perfused with physiological saline and subsequently with 4% paraformaldehyde before preparation of the brains. The brains were equilibrated in a 30% sucrose solution (4 °C, overnight), frozen in M-1 embedding matrix (Shandon, Pittsburgh, PA, USA), and then sectioned on a cryostat. Histochemical analysis of GUSB activity was performed on 20-μm-thick frozen sections using naphthol AS-BI β-D-glucuronide (Sigma) as a substrate [26].

Lysosomal enzyme activities of the neurosphere. Lysosomal enzyme activities in neurospheres, the marrow stromal cells, and human granulocytes were quantified using a fluorometric assay as described with some modification [27].

Histopathological analysis of lysosomal storage. Histopathology in neurons and glia was analyzed at 2 months after transplantation, corresponding to 2 months of age ($n = 2$). Tissues were isolated from the mice and immediately immersed in cold 2% glutaraldehyde in 0.1 M cacodylate buffer, postfixed in 1% osmium tetroxide, dehydrated through a graded series of ethanol solutions, and embedded in Spurr's Medium (Polyscience, Warrington, PA, USA). Toluidine blue-stained, 0.5-μm-thick sections were analyzed for evidence of lysosomal storage in hippocampus, cortex, and ependyma. Cytoplasmic lysosomal distensions in the cortex were also evaluated with an electron microscope.

Auditory brain-stem responses. ABR examination was performed 20 min after anesthesia in a quiet room, as described previously [28].

Novel-object recognition tests. Novel-object recognition tests evaluate nonspatial hippocampus-dependent learning and memory [19–21] and were performed as described [19] with several modifications. The mice were habituated in an open field over a 2-day preexposure (day 1 for 5 min and day 3 for 5 min). Two yellow objects (A and B) were placed diagonally in the open field (15 cm away from the walls) on day 4, and the mice were allowed to explore them for 10 min. Object B was replaced with the novel object (C), and the other object was replaced with a replica (A′) on day 5, and the mice were again allowed to explore them for 10 min. Recognition of the familiar object was scored by preferential exploration of the novel object. A + B represents total time exploring on day 4. A′ + C represents total time exploring on day 5. B/(A + B) represents the ratio of time exploring object B to total time exploring on day 4. C/(A′ + C) represents the ratio of time exploring object C to total time exploring on day 5.

ACKNOWLEDGMENTS

This work was supported by a grant from Terumo Foundation Life Science Foundation to HO, and a grant from the 21st Century COE program of the Japanese Ministry of Education, Culture, Sports, Science and Technology Ministry to Keio University.

RECEIVED FOR PUBLICATION APRIL 27, 2005; REVISED SEPTEMBER 13, 2005; ACCEPTED SEPTEMBER 27, 2005.

REFERENCES

1. Sly, W. S., Quinton, B. A., McAllister, W. H., and Rimoin, D. L. (1973). β-Glucuronidase deficiency: report of clinical, radiologic, and biochemical features of a new mucopolysaccharidosis. *J. Pediatr.* **82:** 249–257.
2. Vogler, C., *et al.* (1993). Enzyme replacement with recombinant beta-glucuronidase in the newborn mucopolysaccharidosis type VII mouse. *Pediatr. Res.* **34:** 837–840.
3. Birkenmeier, E. H., *et al.* (1991). Increased life span and correction of metabolic defects in murine mucopolysaccharidosis type VII after syngeneic bone marrow transplantation. *Blood* **78:** 3081–3092.
4. Snyder, E. Y., Taylor, R. M., and Wolfe, J. H. (1995). Neural progenitor cell engraftment corrects lysosomal storage throughout the MPS VII mouse brain. *Nature* **374:** 367–370.
5. Taylor, R. M., and Wolfe, J. H. (1997). Decreased lysosomal storage in the adult MPS VII mouse brain in the vicinity of grafts of retroviral vector-corrected fibroblasts secreting high levels of β-glucuronidase. *Nat. Med.* **3:** 771–775.
6. Kosuga, M., *et al.* (2001). Engraftment of genetically engineered amniotic epithelial cells corrects lysosomal storage in multiple areas of the brain in mucopolysaccharidosis type VII mice. *Mol. Ther.* **3:** 139–148.
7. Reynolds, B. A., and Weiss, S. (1992). Generation of neurons and astrocytes from isolated cells of adult mammalian central nervous system. *Science* **255:** 1707–1710.
8. Ogawa, Y., *et al.* (2002). Transplantation of in vitro-expanded fetal neural progenitor cells results in neurogenesis and functional recovery after spinal cord contusion injury in adult rats. *J. Neurosci. Res.* **69:** 925–933.
9. Lindvall, O., *et al.* (1990). Grafts of fetal dopamine neurons survive and improve motor function in Parkinson's disease. *Science* **247:** 574–577.
10. Freed, C. R., *et al.* (1992). Survival of implanted fetal dopamine cells and neurologic improvement 12 to 46 months after transplantation for Parkinson's disease. *N. Engl. J. Med.* **327:** 1549–1555.
11. Gwynn, B., Lueders, K., Sands, M., and Birkenmeier, E. H. (1998). Intracisternal A-particle element transposition into the murine β-glucuronidase gene correlates with loss of enzyme activity: a new model for β-glucuronidase deficiency in the C3H mouse. *Mol. Cell. Biol.* **18:** 6474–6481.
12. Lois, C., and Alvarez-Buylla, A. (1994). Long-distance neuronal migration in the adult mammalian brain. *Science* **264:** 1145–1148.
13. Ourednik, V., *et al.* (2001). Segregation of human neural stem cells in the developing primate forebrain. *Science* **293:** 1820–1824.
14. Meng, X. L., Shen, J. S., Ohashi, T., Maeda, H., Kim, S. U., and Eto, Y. (2003). Brain transplantation of genetically engineered human neural stem cells globally corrects brain lesions in the mucopolysaccharidosis type VII mouse. *J. Neurosci. Res.* **74:** 266–277.
15. Tamaki, S., *et al.* (2002). Engraftment of sorted/expanded human central nervous system stem cells from fetal brain. *J. Neurosci. Res.* **69:** 976–986.
16. Sferra, T. J., Backstrom, K., Wang, C., Rennard, R., Miller, M., and Hu, Y. (2004). Widespread correction of lysosomal storage following intrahepatic injection of a recombinant adeno-associated virus in the adult MPS VII mouse. *Mol. Ther.* **10:** 478–491.
17. Kopen, G. C., Prockop, D. J., and Phinney, D. G. (1999). Marrow stromal cells migrate throughout forebrain and cerebellum, and they differentiate into astrocytes after injection into neonatal mouse brains. *Proc. Natl. Acad. Sci. USA* **96:** 10711–10716.
18. Sands, M. S., Erway, L. C., Vogler, C., Sly, W. S., and Birkenmeier, E. H. (1995). Syngeneic bone marrow transplantation reduces the hearing loss associated with murine mucopolysaccharidosis type VII. *Blood* **86:** 2033–2040.
19. Dulawa, S. C., Grandy, D. K., Low, M. J., Paulus, M. P., and Geyer, M. A. (1999). Dopamine D4 receptor-knock-out mice exhibit reduced exploration of novel stimuli. *J. Neurosci.* **19:** 9550–9556.
20. Soderling, S. H., *et al.* (2003). Loss of Wave-1 causes sensorimotor retardation and reduced learning and memory in mice. *Proc. Natl. Acad. Sci. USA* **100:** 1723–1728.
21. Rompon, C., *et al.* (2000). Enrichment induces structural changes and recovery from nonspatial memory deficits in CA1 NMDAR-knockout mice. *Nat. Neurosci.* **3:** 238–244.
22. O'Connor, L. H., *et al.* (1998). Enzyme replacement therapy for murine mucopolysaccharidosis type VII leads to improvements in behavior and auditory function. *J. Clin. Invest.* **101:** 1394–1400.